White Paper

Anritsu Advancing beyond

Surface Shape Measurement by OFDR Using Wavelength Swept Light Source

– Actual Analysis Method and Measurement Examples –

Contents

1 Introduction

Production lines are starting to introduce various sensing technologies due to the rapid progress of digital transformation (DX) in manufacturing industry. The data measured in real time by each of these sensers is analyzed and fed-back to the manufacturing processes to improve productivity and product stability through advances in smart factory automation, which is expected to cut workforce requirements. Conventionally, measurement of product dimensions, displacement and surface roughness on production lines used probes in contact with the product to measure positional displacement. In this case, time is required to move sampled products to the testing location and there is always a risk of mixing out-of-specification products with the production lot. More recently, the advent of smart factories has seen replacement of conventional contact measurement methods by non-contact optical measurements, enabling in-line shape measurement of all products performed previously by sample testing, while also cutting workforce size and improving productivity. Optical non-contact measurement methods are broadly divided into triangulation range finding and 3D scanning methods using continuous wave (CW) light sources, and white-light interferometry methods using white-light sources. Table 1-1 lists optical non-contact measurement methods and the typical specifications. The measurement ranges and accuracies listed in the table are typical values and may vary depending on the product options and grades. The white-light interferometry, Swept Source Optical Coherence Tomography (SS-OCT), Spectral Domain Optical Coherence Tomography (SD-OCT), and Optical Frequency Comb methods feature high accuracy and short measurement range, as well as high-accuracy measurement over a narrow area. However, they suffer from problems when measuring large areas, or hot objects affecting the measurement system or when measuring over longer ranges. The Time of Flight (ToF) method can measure ranges of about 100 m and has been developed mainly for autonomous automobile Light Detection And Ranging (LiDAR) applications, but is unsuitable for industrial quality-inspection applications due to the relatively low measurement accuracy of about 10 cm.

Table 1-1 Optical Non-Contact Measurement Methods and Typical Specifications

Measurement Method	Light Source	Measurement Range	Measurement Accuracy
OFDR	Wavelength Swept light Source	Several meters	Several μm
White-Light Interferometry	White Light Source (SLD, LED, etc.)	1 μm	1 nm
SS-OCT	Wavelength Swept light Source	10 mm	5 μm
SD-OCT	White Light Source (SLD, LED, etc.)	5 mm	5 μm
Optical Frequency Comb	Pulse light Source	6 mm	1 μm
Triangulation Range Finding	CW light Source	~1 m	0.1 mm
Time of Flight (ToF)	Pulse light Source	100 m	10 cm
3D Scanner	CW light Source	~2 m	20 to 50 μm

The measurement range and accuracy of Optical Frequency Domain Reflectometry (OFDR) makes it the ideal method for industrial applications. OFDR is an interference measurement method using a wavelength swept light source, and can measure with an accuracy of several μm at ranges up to several meters. It measures the distance with high accuracy to the target object using the interference signal between the light reflected from the target and the reference light; it is generally described as a Frequency Modulated Continuous Wave (FMCW) technology. OFDR uses wavelength swept light sources where the wavelength of the output optical signal changes with time. When configuring OFDR using a wavelength swept light source, it is important to choose a light source with the best specifications matching the measurement target. For example, to achieve high positional resolution it is necessary to use a light source with a wide wavelength sweep width, while a light source with a high wavelength sweep frequency is required to measure a target moving at high speed in real-time. Additionally, measurement over a wide range requires selection of a laser light source with high coherence. Using a high-coherence light source supports measurement of the OFDR interference signal with a high signal to noise ratio (SNR) which improves the position resolution and accuracy.

Our company has developed and sells wavelength swept light-source models (AQA5500P, AQB5500P, AQA5500D, AQB5500D) that are ideal for OFDR applications. These wavelength swept light sources use the Littman configuration with a Micro Electro-Mechanical System (MEMS) scanning mirror to achieve the following features[1), 2)]:

a. kHz-order high-speed wavelength sweeping
b. High coherence due to single vertical mode narrow-bandwidth laser
c. Mode-hopping (wavelength shift) free, continuous wide wavelength sweep width

Table 1-2 shows the external appearance and list the main specifications of Anritsu's wavelength swept light sources. The product line includes standalone benchtop type and built-in unit type for equipment embedding. Additionally, we have models with two wavelength sweep speeds of 1250 Hz and 150 Hz to meet the measurement requirements of different markets. Please refer to the product catalogs for the detailed specifications of each model.

Table 1-2 Main Specifications of Wavelength Swept Light Source

Item	Specification				Remarks
Model	AQA5500P	AQB5500P	AQA5500D	AQB5500D	-
Type	Benchtop		Built-in unit		-
Appearance					-
Electrical and Optical Features					
Sweep Center Wavelength	1550 ±5 nm				AQA5500P/AQA5500D: At 110 nm sweep AQB5500P/AQB5500D: At 70 nm sweep
Wavelength Sweep Width	30 to 110 nm	15 to 70 nm	30 to 110 nm	15 to 70 nm	Setting Resolution: 1 pm Set from PC software via USB
Sweep Frequency	1250 ±5 Hz	150 ±20 Hz	1250 ±50 Hz	150 ±20 Hz	Fixed non-adjustable value
Average Optical Output Power	≥ 10 mW				CW output

This paper explains surface shape measurement with OFDR are using Anritsu's Wavelength Swept Light Source[3), 4)]. For an explanation of the measurement procedure using OFDR, refer to the Wavelength Swept Light Source technical note and the Anritsu wavelength swept light source product page; this article explains details about important configuration examples, analysis procedures, and settings for shape measurement, as well as methods for compensating measurement problems. Additionally, Chapter 3 presents some actual measurement results for shape measurement of a car body using our wavelength swept light source indicating the possibility of measurement from a long distance of relatively large, manufactured products with µm-order accuracy. In addition, we explain high-accuracy measurement of a fine structure by measuring the shape of a gage block with step differences of 2 µm or less.

2 OFDR Measurement Procedure

This chapter explains the analysis procedure at surface shape measurement using OFDR. Table 2-1 summarizes the processes at each step and the relevant explanation in this chapter.

Table 2-1 OFDR Processing Sequence and Reference chapter

Process	Outline	Section
Measurement Principle	Basic principles of OFDR	2.1
Linearize and Sampling	Compensates for sweep wavelength nonlinearity and improves accuracy of reflected peak waveforms	2.3
Delay Compensation	Matches optical frequency of measurement interferometer and reference interferometer to reduce sidemode after FFT	2.4
Wavelength Dispersion Compensation	Compensates for effect of wavelength dispersion created by measurement system and improves position accuracy of reflected peak waveforms	2.5
Reference Interference Optical Path Length Difference Measurement	Measures reference interferometer optical path length difference and calculates maximum measurement distance range	2.6
Peak Detection	Detects peak position with high accuracy	2.7
Distance Calculation	Converts peak position to distance	2.8

2.1 Measurement Principle

First, this section explains the basic principle of surface shape measurement using OFDR. Figure 2.1-1 shows the basic configuration of a measurement system which is composed of wavelength swept light source, optical interferometer, collimator lens, and optical receiver (balanced receiver). As shown in Fig. 2.1-2(a), the frequency of the light output from the wavelength swept light source is increased linearly over time. The wavelength swept light is split by an optical coupler into the reference optical path L_R and the measurement optical path L_M. The light injected to the reference path passes to the receiver directly. The light split by the coupler and passed to the measurement path passes through an optical circulator and collimator lens before it is emitted into free space to illuminate the measurement target; the light reflected from the target is condensed by the collimator lens and passes through the optical circulator to the optical receiver. The optical coupler in front of the optical receiver combines the light passing through the reference path with the light passed through the measurement path and the optical signal is converted to an electrical signal by the optical receiver. Since these two light paths have different optical path lengths, combining the light passing through these two paths creates a time difference τ, as shown in Fig. 2.1-2(b). This results in the output of an interference signal from the optical receiver with a beat frequency $f_{Beat}[Hz]$ corresponding to the difference in the optical path length $z\,[m]$ between the reference optical path length $L_R\,[m]$ and the measurement optical path length $L_M\,[m]$.

The length of the optical reference path from the wavelength swept light source to the optical receiver (blue line in Fig. 2.1-1) and the length of the measurement path to the collimator lens and from the collimator lens to the optical receiver (red lines in Fig. 2.1-1) are adjusted to the same length using optical fiber so information on the distance of the measurement target from the collimator lens is included in the interference signal $f_{Beat}[Hz]$.

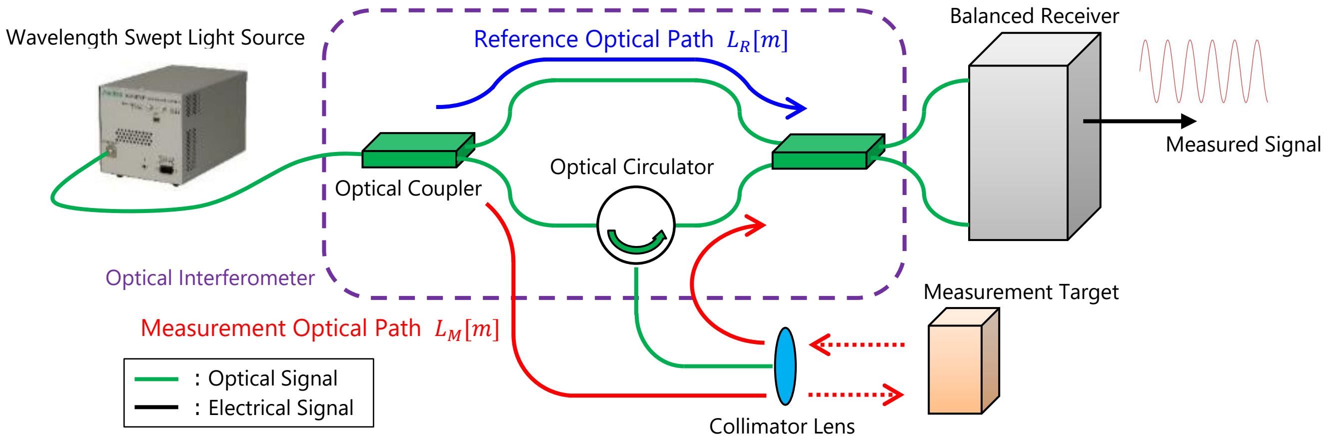

Fig. 2.1-1 Basic Principle of Surface Shape Measurement by OFDR

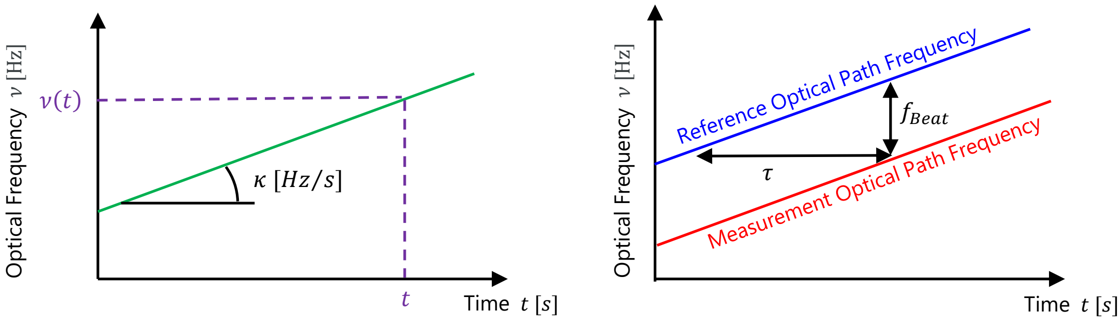

(a) Temporal Change in Frequency of Optical Output from Wavelength Swept Light Source

(b) Temporal Change in Optical Frequency Observed at Optical Receiver

Fig. 2.1-2 Temporal Change in Optical Frequency

When the frequency of the optical output from the wavelength swept light source changes linearly with time as shown in Fig. 2.1-2(a), the optical frequency $\nu(t)$ at time t is found as follows:

$$\nu(t) = \nu_0 + \kappa \cdot t \qquad (1)$$

where, $\nu_0[Hz]$ is the optical frequency at time 0, and $\kappa[Hz/s]$ is the optical frequency sweep speed. When the difference in the length of the reference and measurement optical paths is z [m], and the difference in the propagation time created by both paths is τ [s], each value is found using the following equations using the reference optical path length L_R [m] and measurement optical path length L_M [m] referenced to the refractive index and the velocity of light in vacuum c [m/s].

$$z = |L_M - L_R| \qquad (2)$$

$$\tau = \frac{|L_M - L_R|}{c} = \frac{z}{c} \qquad (3)$$

In addition, when the electrical field strength of the light passing via the reference optical path and measurement optical path is E_R and E_M, respectively, the interference power P detected at the optical receiver is found as follows:

$$\begin{aligned} P &= \left|\overrightarrow{E_R} + \overrightarrow{E_M}\right| \\ &= \left|E_R e^{-i2\pi\nu t \cdot t} + E_M e^{-i2\pi\nu(t-\tau)\cdot t}\right|^2 \\ &= |E_R|^2 + |E_M|^2 + 2|E_R||E_M| \cos\left(2\pi \frac{\kappa z}{c} t\right) \qquad (4) \end{aligned}$$

The third derivation in Eq. (4) is observed by removing the DC components of the interference signal. In other words, as shown in Eq (1), sweeping the optical frequency linearly outputs the optical signal frequency expressed by Eq. (5) from the optical receiver.

$$f_{Beat} = \frac{\kappa z}{c} \qquad (5)$$

From Eq. (5), it is clear that the interference signal frequency f_{Beat} is dependent on the difference in the length of the optical paths z.

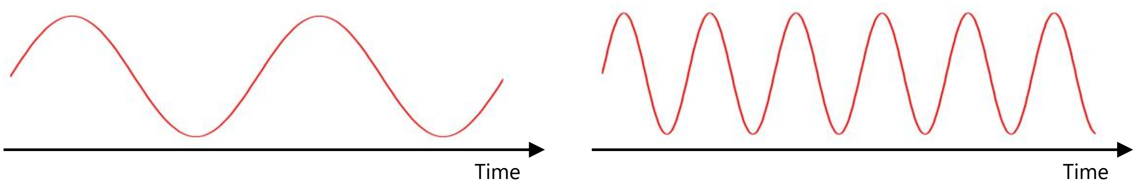

(a) Example of Interference Signal with Short Optical Path Length Difference

(b) Example of Interference Signal with long Optical Path Length Difference

Fig. 2.1-3 Example of interference signal f_{Beat} observed by receiver

When sweeping from short to long wavelengths linearly over time, the optical frequency display has a reverse gradient.

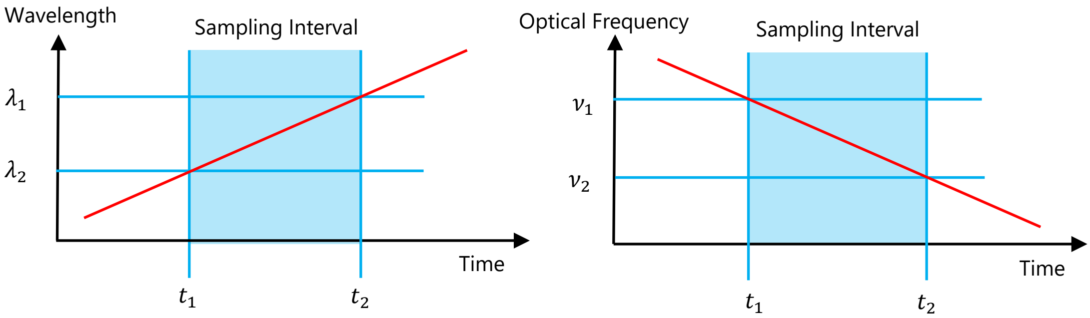

(a) Sampling interval on wavelength axis (b) Sampling interval on frequency axis

Fig, 2.1-4 Explanation of Sampling Interval

When sampling the interference signal f_{Beat} output from the optical receiver from time t_1 to t_2, the number of waves *M* of the interference signal observed in the sampling interval is expressed by Eq. (6).

$$M = f_{Beat}(t_2 - t_1) = \frac{\kappa z}{c}(t_2 - t_1) \qquad (6)$$

where the sweep speed $\kappa[Hz/s]$ is expressed by Eq. (7)

$$\kappa = \frac{\nu_1 - \nu_2}{t_2 - t_1} = \frac{\frac{c}{\lambda_1} - \frac{c}{\lambda_2}}{t_2 - t_1} \cong \frac{c\Delta\lambda}{\lambda_c^2(t_2 - t_1)} \qquad (7)$$

Here, $\Delta\lambda = \lambda_2 - \lambda_1$ is the wavelength sweep width, and λ_c is the sampling center wavelength. Accordingly, the number of waves *M* of the interference signal observed in the sampling interval is expressed by Eq. (8).

$$M = \frac{\Delta\lambda}{\lambda_c^2} z \qquad (8)$$

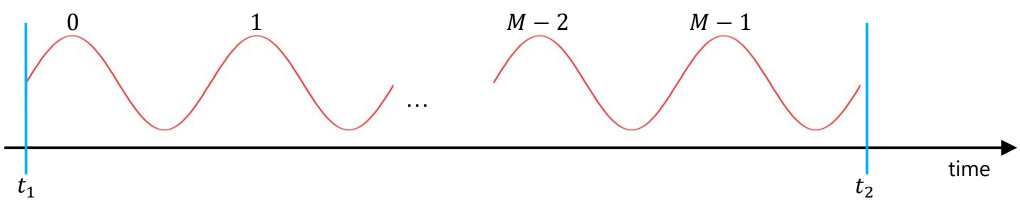

Fig. 2.1-5 Example of Sampled Interference Signal

The relationship between sampling frequency and sample number is shown below. When the sampling frequency is f_s, Eq. (9) expresses the sampled number N from time t_1 to t_2.

$$N = f_s(t_2 - t_1) \qquad (9)$$

Consequently, the sampled number is expressed by Eq. (10) derived from Eq. (7) and Eq. (9).

$$N = f_s \frac{c\Delta\lambda}{\kappa\lambda_c^2} \qquad (10)$$

The M peak position can be observed by applying Fast Fourier Transformation (FFT) to the sample data. However, when the A/D conversion bandwidth is wide and the sampling frequency f_s is large, since the measurement bandwidth becomes wider as f_s becomes larger, longer distances can be measured with no effect on the position of the M reflection peak.

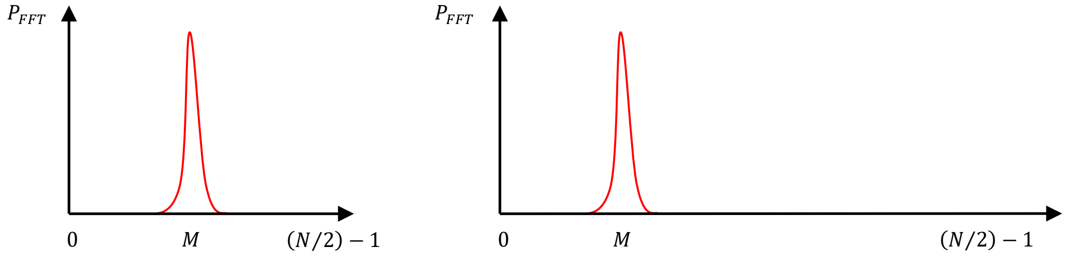

(a) At small f_s (small N) (b) At large f_s (large N)

Fig. 2.1-6 Examples of Results After FFT Depending on Size of f_s

The measurement resolution can be expressed as follows. When the position of the measurement target from the collimator lens shown in Fig. 2.1-1 is shifted by dz the interference signal wave number M' is expressed by Eq. (11) derived from Eq. (8).

$$M' = \frac{\Delta\lambda}{\lambda_c^2}(z + 2dz) \qquad (11)$$

In this case, since the incident distance from the collimator lens to the measurement target and the distance of the light reflected from the measurement target to the collimator lens are added to the optical path length difference (z in Eq. (8)) for the optical return journey, twice dz is added in Eq. (11) above. Since the interference signal wave number is an integer value, the measurement resolution is calculated by making the difference between M and M' the minimum value of 1 as shown in Eq. (12).

$$M' - M = \frac{2\Delta\lambda}{\lambda_c^2}dz = 1$$

$$dz = \frac{\lambda_c^2}{2\Delta\lambda} = \frac{c}{2\Delta\nu} \qquad (12)$$

In other words, the measurement resolution is inversely proportional to the wavelength sweep width $\Delta\lambda$ in the sampling interval.

For example, when measuring at a center wavelength of 1550 μm and a wavelength sweep width of 20 nm (2.6 THz), the calculated theoretical resolution is 60 μm. In other words, when plotting distance on the x-axis and reflected power after FFT P_{FFT} on the y-axis, a reflection peak with a peak width of 60 μm is detected at the position of the distance to the measurement target.

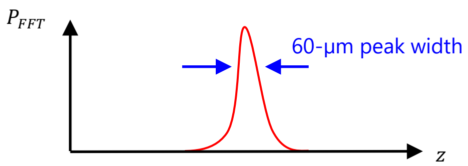

Fig. 2.1-7 Measurement Resolution

The next section explains the relationship between the measurable distance to the measurement target and the measurement system. When the distance from the collimator lens to the measurement target is short, the difference z between the reference optical path length and the measurement optical path length becomes small and a lower interference signal frequency is observed following Eq. (5); the peak position measurement result after FFT is also observed at a nearer distance (Fig. 2.1-8(a)). When the distance from the collimator lens to measurement target is long, the difference z between the reference optical path length and the measurement optical path length becomes long and a higher interference signal frequency is observed; the peak position measurement result after FFT is also observed at a further distance corresponding to the distance difference (Fig. 2.1-8(b)). Consequently, since the interference signal frequency becomes higher as the optical path length difference z becomes longer, the measurable distance is limited by the measurement system bandwidth, such as the optical receiver and A/D conversion board. Moreover, when the optical path length difference z is longer than the coherence, since the correlation between the light passing via both paths is lost, the coherence length of the light source is also an important factor. When the optical path length difference z is longer than the coherence length, the peak line width after FFT becomes almost as wide as the line width of the laser itself, resulting in a very degraded peak detection accuracy. As shown in Fig. 2.1-8(c), since the optical path length difference z must consider the return journey distance to the measurement target, this phenomenon occurs obviously if the distance from the collimator lens to the measurement target is equivalent to a distance of at least half the coherence length. As a consequence, when the distance to the measurement target is long, not only must the bandwidth of the optical receiver and A/D conversion be improved, but also selection of a light source with long coherence is necessary. Our wavelength swept light sources have high coherence due to use of a single vertical-mode, narrowband laser and are the optimum laser light sources for OFDR measurement.

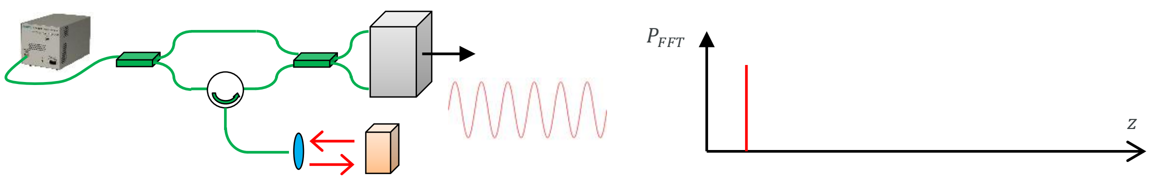

(a) Short Optical Path Length Difference z

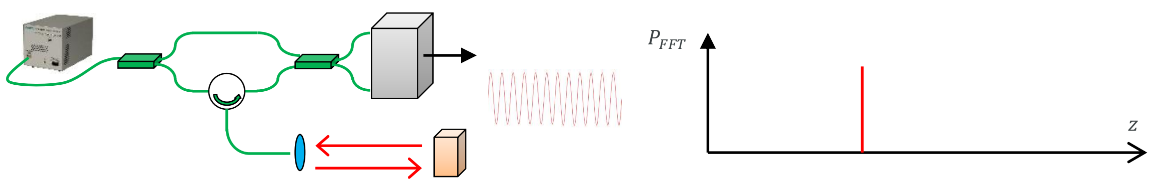

(b) Long Optical Path Length Difference z

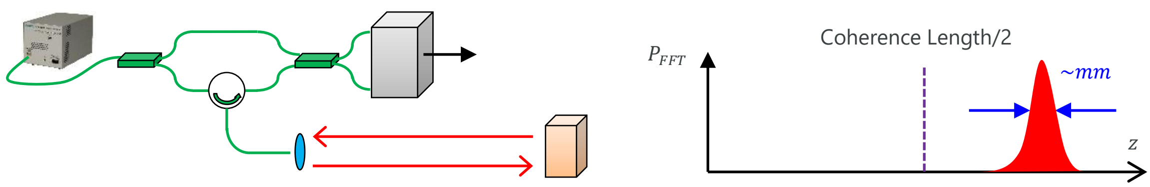

(c) When Optical Path Length Difference z More Than Coherence Length

Fig. 2.1-8 Relationship Between Measurable Distance and Measurement System

2.2 Examples of Interferometer Configurations

Figure 2.1-1 showed the structure of a Mach-Zehnder interferometer as a typical example of a configuration for OFDR. This section provides a simple explanation of other configuration examples. Figure 2.2-1(a) shows an example of the Michelson interferometer configuration. In this example, although the design has the advantage of reducing the number of optical couplers and optical circulators, there are challenges using an optical balanced receiver, and the disadvantage is that it is impossible to filter AM noise in the interference signal. Figure 2.2-1(b) shows the structure of a Mach-Zehnder interferometer like that in Fig. 2.1-1, but it is configured without using an optical circulator. Generally, an optical circulator is more expensive than an optical coupler, but it is difficult to implement a wider wavelength bandwidth due to the large impact of the wavelength dependency of the built-in Faraday element. According to Eq. (12), due to the dependence of the OFDR measurement resolution on the wavelength sweep width, restricting the usable wavelength range is linked to reduced resolution. As a result, the structure of the type of Mach-Zehnder interferometer shown in Fig. 2.2-1(b) has the merits of simplicity, wavelength bandwidth, and cost. Moreover, since a balanced receiver can be used as the optical receiver, the configuration is also effective for filtering AM noise. However, since some of the light reflected by the measurement target returns to the wavelength swept light source, it suffers from the disadvantage of large optical loss.

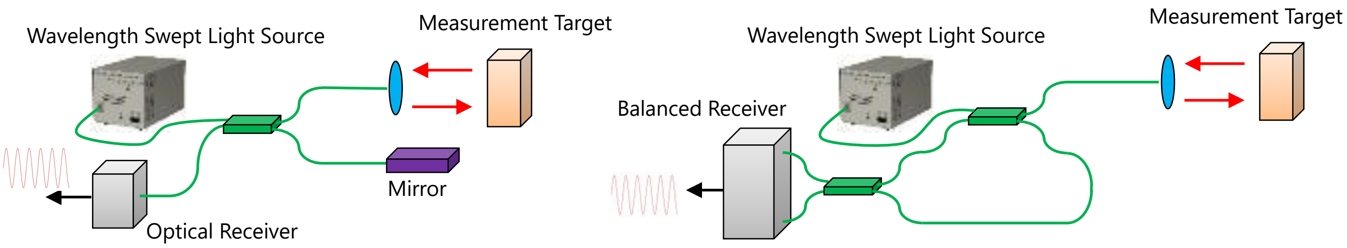

(a) Configuration Using Michelson Interferometer (b) Configuration Using Mach-Zehnder Interferometer

Fig. 2.2-1 Examples of Interferometer Configuration

2.3 Linearize Processing and Sampling

When the relationship between the change in wavelength and time is linear, the frequency of the interference signal output from the optical interferometer is constant and the FFT result produces a peak at a position matching this frequency (Fig. 2.3-1(a)). However, generally, since the change in the wavelength of the light output from wavelength swept light sources is non-linear, the interference signal frequency changes with time, resulting in a wide peak after FFT analysis (Fig. 2.3-1(b). For example, the wavelength sweep of our light sources is sinusoidal over time and the nonlinearity is especially noticeable near the part where the wavelength returns (Fig. 2.3-2). When wavelength sweeping is nonlinear, the peak position becomes difficult to differentiate because a wide peak is observed after FFT. Therefore, in addition to the measurement path including the measurement target, it is important to compensate the effect of nonlinearity by using a reference interferometer. This section describes the linearize processing for making this compensation using a reference interferometer.

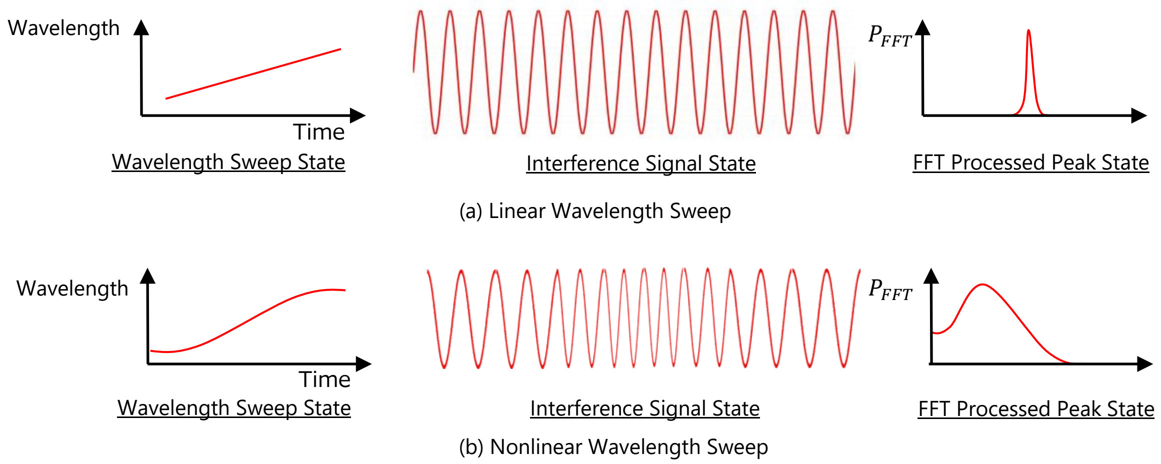

Fig. 2.3-1 Examples of FFT Analysis Results vs Sweep Wavelength Linearity

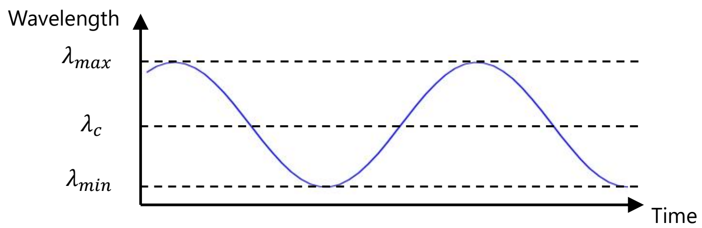

Fig. 2.3-2 Anritsu Wavelength Swept Light Source Optical Output Wavelength State

Figure 2.3-3 shows an example of a measurement system using a reference interferometer. The optical output from the wavelength swept light source is split by an optical coupler. The light input to the reference interferometer is input to a Michelson interferometer designed with an optical path length difference L_{AUX}. After reflection by the Faraday mirror in the Michelson interferometer, the reference signal with a frequency corresponding to the optical path length difference L_{AUX} is output from the optical receiver. Section 2.2 describes the advantages of the Mach-Zehnder interferometer but there are challenges in designing this Mach-Zehnder configuration using a Faraday mirror. However, by using a Faraday mirror as the reflection mirror, since the light from each reflection mirror can be input to the optical receiver in the same polarization state irrespective of the optical path length difference, the system has the advantage of being able to eliminate changes in the interference signal due to the polarization state. Here, since the priority is eliminating the effect of polarization changes, the Michelson interferometer structure uses a Faraday mirror. Additionally, as shown in Fig. 2.3-3, the reference interferometer and measurement interferometer are constructed entirely from single mode fiber (SMF). Although it is possible to propagate light in either the slow or fast axis to the measurement interferometer collimator lens by using Polarization Maintaining Fiber (PMF) when concerned about the effect of polarization state changes, but when emitted in free space, the polarization state of the light incident to the measurement target changes according to the incident angle to the measurement target. Consequently, it is difficult to re-couple the light in the collimator lens with linear polarized light. As a result, the light is propagated in the section between the collimator lens and optical receiver using both the slow and fast axes. Since each axis has a different refractive index, the measured signal is split, and two peaks are observed in the finally captured FFT spectrum. To suppress this, as shown in the system configuration in Fig. 2.3-3, SMF is used throughout the entire optical system. Ideally, it would be best to compensate the polarization changes using a polarization diversity configuration, but there are problems with the complexity and high cost of such a design. In the measurement interferometer shown below, the polarization state is tuned by adjusting the angle of the fiber near the collimator lens to measure the power of the reflected light at a fixed position where it is strongest.

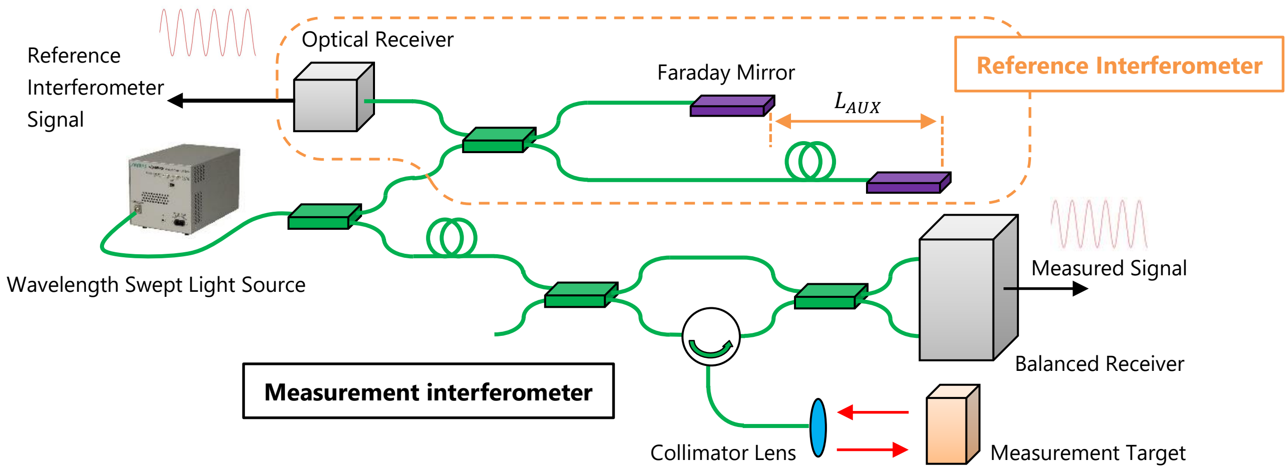

Fig. 2.3-3 OFDR Measurement System using Reference Interferometer

There are hardware linearize processing and software linearize processing as a method of compensating the non-linearity of wavelength sweep using a reference interferometer. The former method synchronizes with a reference interference signal input to the sampling clock of the A/D conversion board and samples the measured signal. Therefore, it has the advantage of simple calculation processing. Moreover, since only the signal synchronized to the rising reference signal is sampled, a wide bandwidth of the A/D conversion board can be used. As a result, the reference interference signal frequency can be widened to near the A/D conversion board bandwidth to support setting of longer distances to the measurement target. Furthermore, since it eliminates the need for complex sampling calculation processing, there is also the advantage of reduced PC loads. However, an A/D conversion board is required for input of the reference interferometer signal as the sampling clock.

The latter software linearize processing method samples the reference interference and measured signals at the A/D conversion board before sampling again by calculation processing to compensate the wavelength sweep nonlinearity. Since software linearize processing uses the A/D conversion board internal clock, it has the advantage of supporting general-purpose A/D conversion boards. Moreover, as described later, it also has the advantages of supporting delay compensation (section 2.4) using differences in the lengths of the reference interference signal and measured signal fiber lengths, as well as performing calculation processing for compensating wavelength dispersion (section 2.5), but conversely, this has the disadvantage of requiring complex calculations and long computation times imposing heavy loads on the PC. The exact details of each method are explained below.

2.3.1 Hardware Linearize Processing

Hardware linearize processing is a method for sampling the measured signal based on the reference interference signal. From equation (5), the reference interferometer with frequency f_{AUX} represented by equation (13) below is output from the reference interferometer.

$$f_{AUX} = \frac{2\kappa\Delta L_{AUX}}{c} \tag{13}$$

ΔL_{AUX} is the optical path length difference of the reference interferometer including the refractive index of the fiber (see Fig. 2.3-3). In equation (13), the optical path length difference in the reference interferometer is the round trip of ΔL_{AUX} in comparison to previously described Eq. (5), it is expressed as twice the optical path length difference. The Free Spectrum Range (FSR) of the interferometer, in other words the optical frequency required for the interference signal to change by one sine wave period, is expressed as follows:

$$FSR = \frac{c}{2\Delta L_{AUX}} \tag{14}$$

Accordingly, Eq. (13) can be rewritten as follows:

$$f_{AUX} = \frac{\kappa}{FSR} \tag{15}$$

where, the right-hand side of Eq. (15) expresses "how many times the sweep rate κ corresponds to FSR". In other words, f_{AUX} can be said to be "the frequency of the interference signal that maximizes each time the optical frequency is swept by the FSR". If the measurement signal is sampled every time the interference signal becomes maximum or every time the interference signal rises, the measurement signal is sampled every time the optical frequency is swept by FSR. As a result, it is the same as sampling at constant optical frequency intervals. In actual measurement, the reference interference signal is input to the sampling clock of the A/D conversion board, and the measurement signal is input to the channel for acquiring measurement data, and the A/D conversion board samples each time the reference interference signal rises. Therefore, it is possible to sample at a constant optical frequency. By performing an FFT on this sampled data, it is possible to obtain a sharp reflection peak with the effect of non-linearity compensated. As mentioned above, this hardware linearize processing requires an A/D conversion board that can input the reference interference signal as a sampling clock, but the system is simple and does not require complicated arithmetic processing, so the speed is increased. Therefore, it is a technology mainly used for OCT (Optical Coherent Tomography). Performing FFT on this sampled data captures the sharp reflection peaks where the impact of nonlinearity has been corrected. As described previously, although performing this hardware linearize processing requires an A/D conversion board for inputting the reference interference signal as a sampling block, the speed can be easily increased due to the system simplicity and lack of complex processing. As a result, this technology is used mainly for Optical Coherence Tomography (OCT).

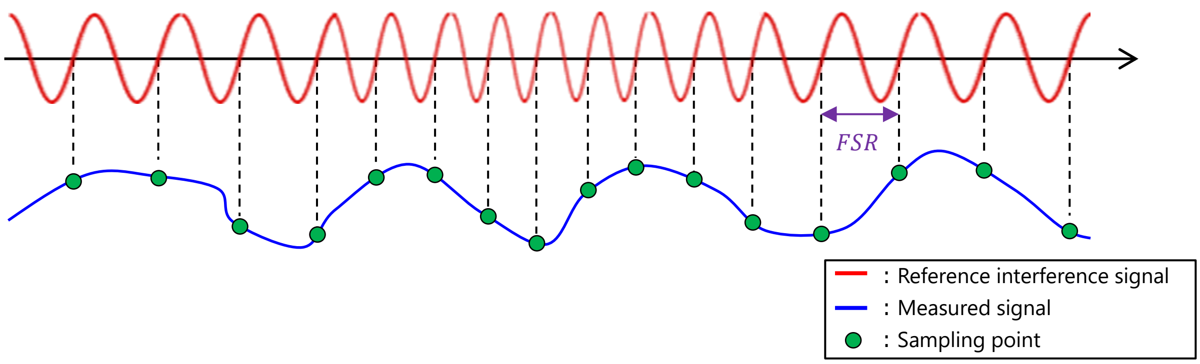

Fig. 2.3.1-1 Hardware Linearize Processing Concept

Where, the measurement resolution is considered from the reference interference signal. When the optical frequency is swept from ν_1 to ν_2, assuming that the number of waves output from the reference interferometer is N, it is expressed as follows.

$$N = \frac{(\nu_1 - \nu_2)}{FSR} = \left(\frac{1}{\lambda_1} - \frac{1}{\lambda_2}\right)\frac{c}{FSR} \qquad (16)$$

Our wavelength swept light source has a built-in etalon based on the optical frequency, and by sampling the etalon signal at the same time as the reference interference signal, the optical frequency during sweep can be measured accurately. Therefore, ν_1 and ν_2 in the above equations can be measured with high accuracy, and ΔL_{AUX} can be expressed as follows from equations (14) and (16).

$$\Delta L_{AUX} = \frac{cN}{2(\nu_1 - \nu_2)} = \frac{N\lambda_1\lambda_2}{2(\lambda_2 - \lambda_1)} \qquad (17)$$

The position of the maximum frequency when the sample data is FFT analyzed is equivalent to ΔL_{AUX} and the position of the reflection point can be found by proportional calculation from the detected peak frequency position. The measurement resolution Δz of the reflection point position can be calculated as follows by dividing by the number N of reference interference signal waves expressed as an integer value from Eq. (17).

$$\Delta z = \frac{c}{2(\nu_1 - \nu_2)} = \frac{1}{2}\frac{\lambda_1\lambda_2}{\lambda_2 - \lambda_1} \simeq \frac{1}{2}\frac{\lambda_c^2}{\Delta\lambda} \qquad (18)$$

where, λ_c is the sweep center wavelength, and $\Delta\lambda$ is the wavelength sweep width.

The optical path length difference L_{AUX} of the reference interferometer must be determined by considering the distance to the measurement target. For example, when the distance from the collimator lens to the measurement target is 10 m, the return optical path length difference becomes 20 m. At this time, the reference interferometer optical path length difference L_{AUX} must be twice 20 m (40 m for return) from the viewpoint of the Nyquist frequency at FFT analysis, which requires a light source with a coherence length of 40 m.

When the frequency of the light output from the wavelength swept light source changes linearly with time as shown in Fig. 2.1-1(a), as described previously, the sweep speed $\kappa[Hz/s]$ is expressed by Eq. (7). The sweep wavelength of Anritsu's wavelength swept light sources changes sinusoidally with time as shown in Fig. 2.3-2. In this case, the sweep rate $\kappa[Hz/s]$ is considered as follows, taking into account the influence of the sweep wavelength that changes in a sinusoidal state. The wavelength $\lambda(t)$ output at time t when the output wavelength is changing sinusoidally is expressed as follows:

$$\lambda(t) = \lambda_0 + \frac{w}{2} \cdot \sin(2\pi f t) \qquad (19)$$

where, $\lambda_0[nm]$ is the optical wavelength at time 0, $w[nm]$ is the wavelength sweep width, and $f[Hz]$ is the sweep frequency. The wavelength sweep speed can be obtained as follows by differentiating Eq. (19).

$$\kappa = \frac{d\lambda(t)}{dt} = 2\pi f \cdot \frac{w}{2} \cdot \cos(2\pi f t) \qquad (20)$$

The maximum sweep speed is at the sweep center position where $\cos(2\pi f t) = 1$. Accordingly, the maximum sweep speed $\kappa_{max}\ [Hz/s]$ is expressed as follows:

$$\kappa_{max} = 2\pi f \cdot \frac{w}{2}$$

$$= \pi f w \qquad (21)$$

The reference interference signal frequency can be calculated from $\kappa_{max}\ [Hz/s]$ in Eq. (21) and from the FSR value using Eq. (15).

Figure 2.3.1-2 shows an example of the compensation effect using hardware linearize processing. This figure shows the transmission spectrum from the etalon and the received light reflected from the measurement target as the interference signal. Figure 2.3.1-2(a) shows the measurement results sampled without linearize processing (equal time interval); Fig. 2.3.1-2(b) shows the measurement result sampled by hardware linearize processing. The measurement target is positioned 1 m from the collimator lens. The reference interferometer fiber length is 8 m and the wavelength sweep width is set to 20 nm. As a result, the theoretical resolution is 60 µm. As shown in Fig. 2-3-2, the shape of the wavelength sweeping of our light source is sinusoidal, resulting in a drop in sweep speed further from the sweep center. Consequently, when measuring at equal time intervals (Fig. 2.3.1-2(a)), the etalon intervals become wider, while they should be at equal optical frequency intervals when getting further from the sweep center (sampling no. = 80,000). On the other hand, the etalon signal peaks are displayed at almost equal intervals in data measured using hardware linearize processing since sampling is performed at equal frequency intervals.

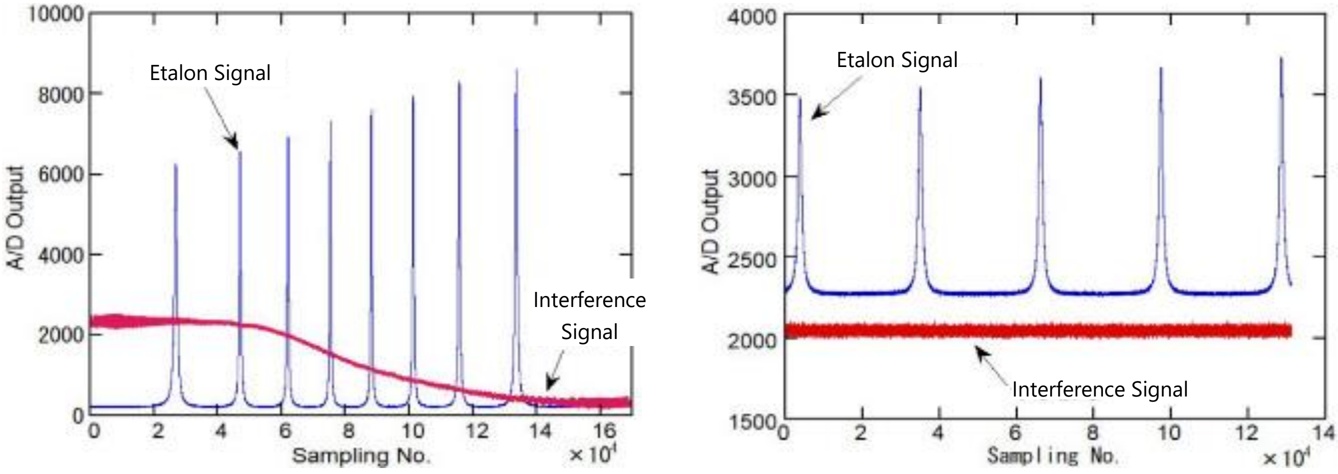

(a) Without Hardware Linearize Processing　　(b) With Hardware Linearize Processing

Fig. 2.3.1-2　Comparison of Etalon Signal Measurement Results

2.3.2　Software Linearize Processing

The software linearize processing method resamples the measured signal based on the reference interference signal phase information after sampling the reference interference signal and measurement signal simultaneously. The Hilbert Transformation is used as a digital filter to calculate the phase data. The Hilbert Transformation is a method for finding the complex variable $z(t)$ by calculating the signal $y(t)$ with 90° delayed phase data for the target signal. The phase data $\varphi(t)$ is calculated from the complex variable $z(t)$.

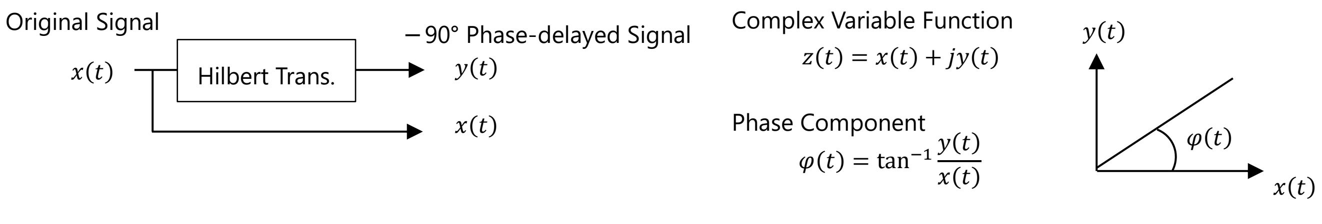

Fig. 2.3.2-1　Hilbert Transformation Concept

Figure 2.3.2-2(a) shows the reference interference signal and Fig. 2.3.2-2(b) shows the reference interference signal phase data calculated using the Hilbert Transformation. The reference interference signal phase changes from $-\pi$ to $+\pi$, increasing and decreasing by 2π between $+\pi$ and $-\pi$. The continuous phase change shown in Fig. 2.3.2(c) is obtained by continuously connecting the 2π decrease using a process known as a Unwrap.

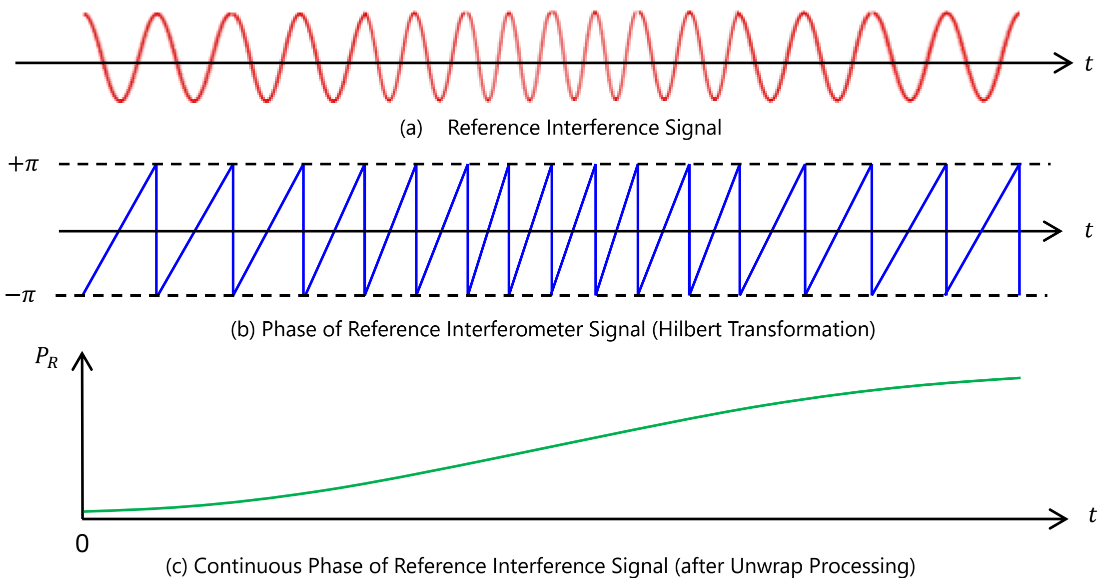

Fig. 2.3.2-2 Reference Interference Signal and Phase

The continuous phase of the reference interference signal obtained in Fig. 2.3.2-2 (c) above is divided into equal intervals, and the measurement signal at the division time is extracted. Then, since FFT analysis will be performed on the divided data, the data is divided into powers of 2 to be appropriate for FFT analysis. As a result, it is equivalent to the optical-frequency data measured at equal intervals. Performing FFT analysis on this resampled data displays peaks at the frequency position proportional to $z(= L_M - L_R)$.

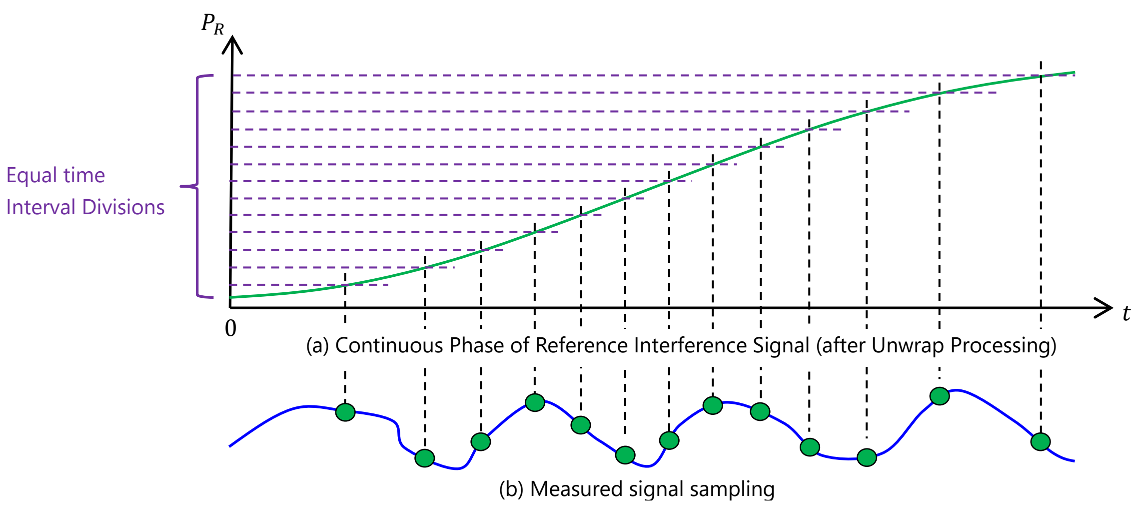

Fig. 2.3.2-3. Software Linearize Sampling Concept

When resampling the measured signal at the phase divided times, the required data can be extracted by interpolating one point from the two measured data points on either side.

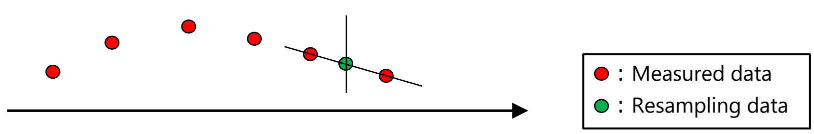

Fig. 2.3.2-4 Interpolation Concept

2.4 Delay Compensation

In the actual measurement, the phase component of the light output from the light source is modulated. Therefore, when there is a difference between the optical path length of the reference interferometer and the measurement interferometer, a time difference occurs in the propagation times of both interferometers, so that the influence of phase modulation remains in the data after linearization. As a result, sidemodes appear at frequency-separated positions of phase modulation (see Figure 2.4-1). When the optical path lengths of both optical paths are the same and there is no difference in propagation time, even if the phase of the light output from the light source is modulated, it can be corrected by a series of linearization processes. Accordingly, the propagation time from the wavelength swept source via the reference interferometer to the input to the A/D conversion board must match the propagation time via the measurement system to the input to the A/D conversion board. Strictly speaking, the average length of the reference interferometer paths A and B must match the average length of the measurement interferometer paths C and D. This can be resolved by inserting a fiber with a length equivalent the reference interferometer optical path length difference $\boldsymbol{2L_{AUX}}$ in front of the measurement interferometer. Inserting a delay-compensation optical fiber matches the optical frequencies at the two optical receivers of the reference interferometer and measurement interferometer to achieve high-accuracy linearize processing. Strictly speaking, successful sampling can be achieved only at the point when the average length of the reference interferometer A and B paths and the time difference to the measurment target are equal; if there are many reflection points, it is difficult to match the optical path lengths at all reflection points.

At hardware linearize processing, inserting the delay-compensating optical fiber as explained above supports some degree of compensation. When more precise correction is required, compensation is possible using the same calculation as described for software linearize processing. When using software linearize processing, it is possible to compensate using the above calculation processing to shift the delay time, which eliminates the need for optical fiber. However, inserting optical fiber at software linearize processing has no impact on the calculation results.

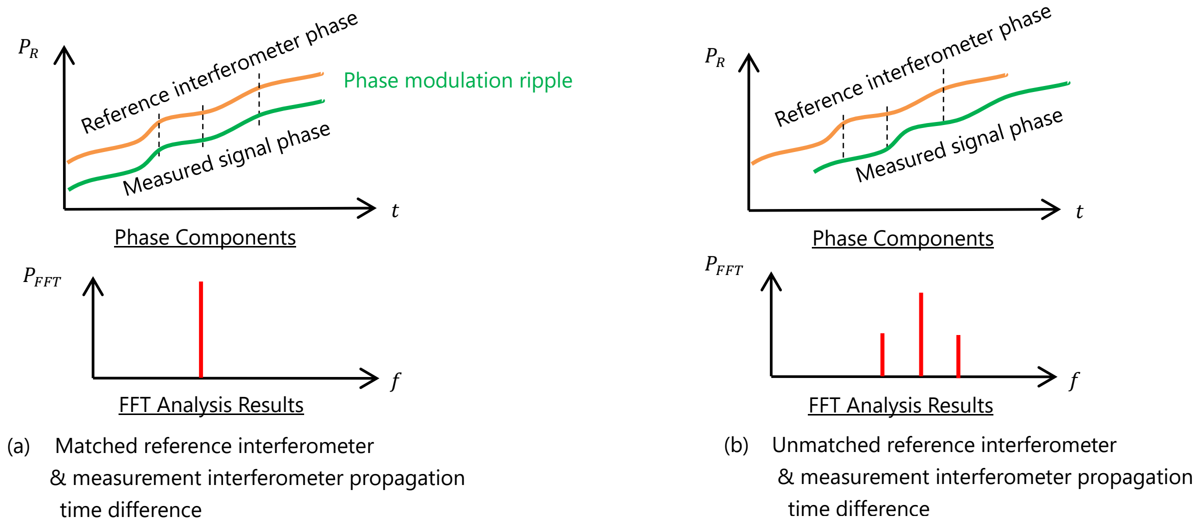

Fig. 2.4-1 Example of Phase Modulation Effect

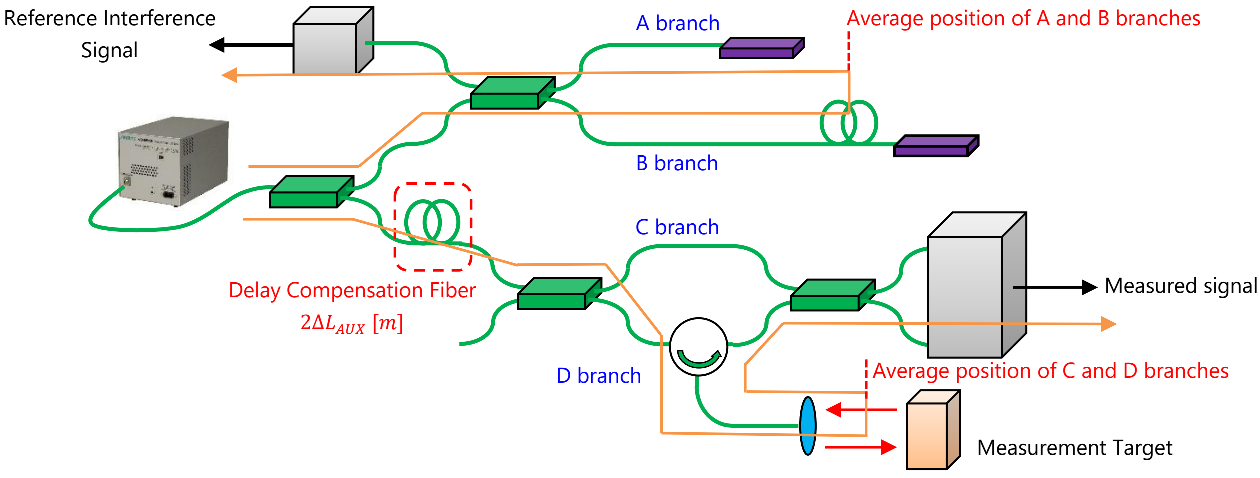

Fig. 2.4-2 Example of OFDR Measurement System with Delay Correction

2.5 Wavelength Dispersion Compensation

Generally, interferometers constructed using optical fiber and free space have wavelength dispersion, which can be a cause of degraded precision. When an interferometer is constructed entirely of optical fiber, the effects of wavelength dispersion created by the reference interferometer and by the measurement interferometer are cancelled. However, with an interferometer constructed of optical fiber and free space, the wavelength dispersion effects are not cancelled and can be a cause of degraded accuracy. Moreover, the same effect can be created even by connecting optical fibers with different core diameters. For example, in an interferometer composed of an optical fiber and a spatial system, when a reference interferometer is configured using an optical fiber whose refractive index increases as the wavelength increases, the effective optical path length on the long wavelength side is longer than that on the short wavelength side. When converted to the optical frequency axis, the interval between optical frequencies becomes narrower toward the longer wavelength (low frequency) side. As a result, when compensating using software linearize processing for example, when dividing the above-described continuous phase $\boldsymbol{P_R}$ into equal intervals, the width of the peak observed after FFT processing becomes even wider. In addition, when there is wavelength dispersion, the FFT peak frequency may also drift, depending on the sampling region (Fig. 2.5-1).

The degree of the wavelength dispersion effect changes even when setting the wavelength sweep width and is smaller when the wavelength sweep width is narrower.

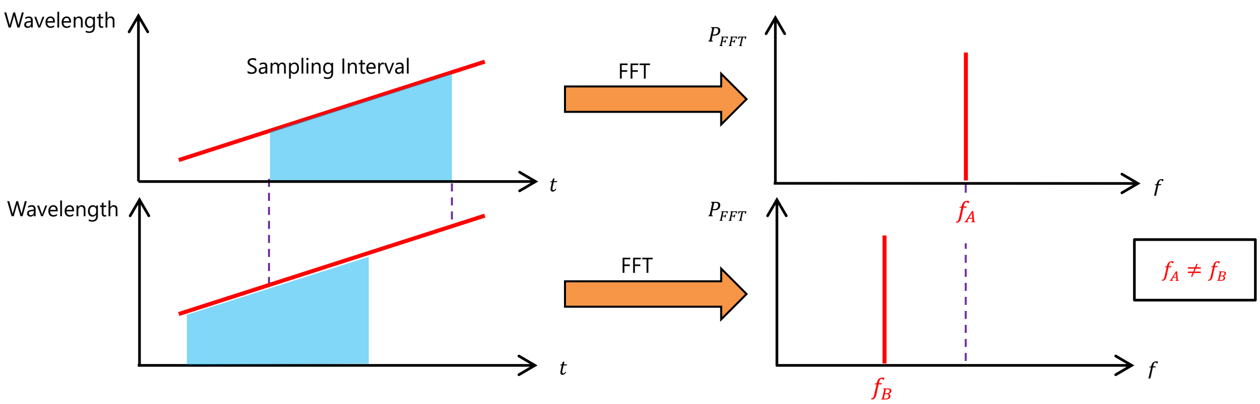

Fig. 2.5-1 Effect of Wavelength Dispersion on Sampling Interval

When measuring using software linearize processing, removing the effect of wavelength dispersion requires calibration. There are two methods: 1. Using the transmission spectrum from a gas cell, and 2. Using the transmission spectrum from an etalon. Generally, the gas cell has a fixed absorption peak wavelength for the input light. The transmitted light from the gas cell is received by the optical receiver where it is converted to an electrical signal for use as the wavelength reference. Similarly, the etalon transmission spectrum can be used as the wavelength reference. This etalon transmission spectrum is received by an optical receiver like the interference signal where it is converted to an electrical signal for use as the wavelength reference. Our wavelength swept light sources have a built-in etalon and output the O/E converted signal. This section focuses on the calibration method using the transmission spectrum from a gas cell. However, calibration using an etalon transmission spectrum is basically the same.

Figure 2.5-2 shows an example of a measurement system using a gas cell. It uses the configuration in Fig. 2.4-2 with an inserted gas cell. Figures 2.5-3 and 2.5-4 show the calibration procedure. First, the phase $\boldsymbol{P_R}$ of the reference interferometer after unwrapping is found by sampling at the same time interval as the gas cell absorption peak frequency $\boldsymbol{f_e}$. The fourth-order fitting function is used here. Next, the gas cell peak frequency $\boldsymbol{f_e}$ is plotted on the x-axis and the reference interferometer phase $\boldsymbol{P_R}$ is plotted on the y-axis and sorted to find the $\boldsymbol{P_R}$ function by fourth-order fitting.

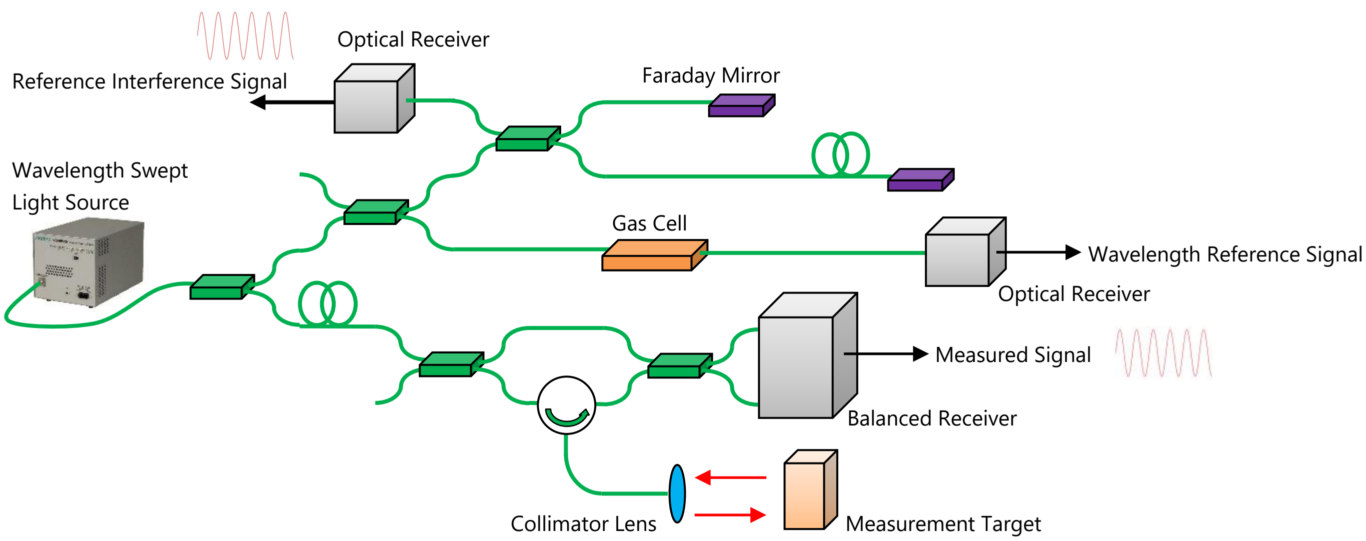

Fig. 2.5-2 Example of Measurement System Using Gas Cell

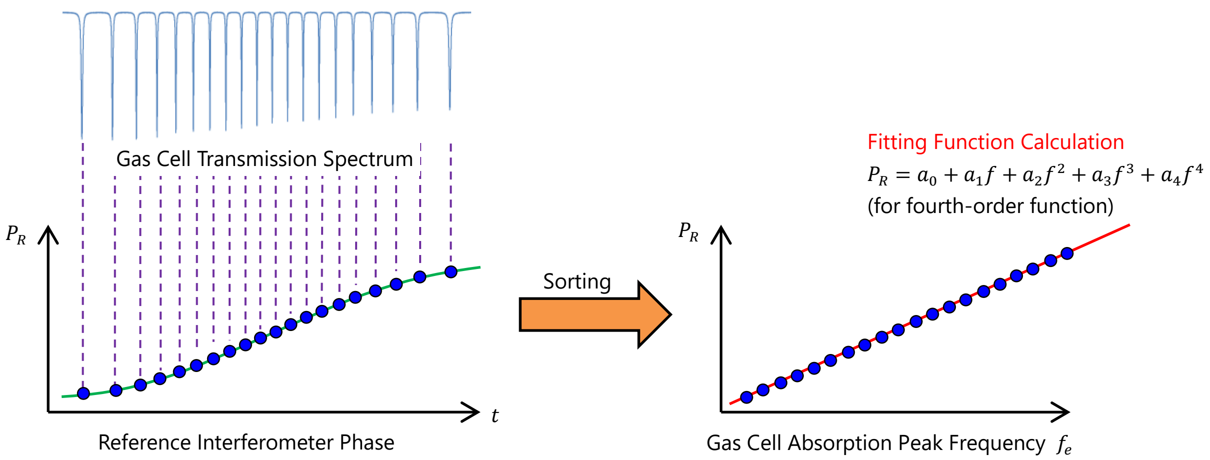

Fig. 2.5-3 Sampling Using Gas Cell Absorption Peak Wavelength Time

For the phase P_R, of the reference interference signal in which the absorption peak frequency f_e of the gas cell is rearranged on the horizontal axis in Fig. 2.5-3, the optical frequency (horizontal axis) is divided at equal intervals, and P_R at each optical frequency is calculated from the fitting function (see Figure 2.5-4 (a)). For example, P_R was calculated at intervals of 0.0572 GHz by sampling at a wavelength sweep width of 30 nm (about 3750 GHz) and dividing into 65,536 parts (2^{16}). Then, since FFT analysis will be performed on the divided data, the data is divided into powers of 2 to be appropriate for FFT analysis. Next, the signal measured at the calculated P_R is extracted and subjected to FFT to calculate the calibrated result for the impact of wavelength dispersion (Fig. 2.5-4(b).

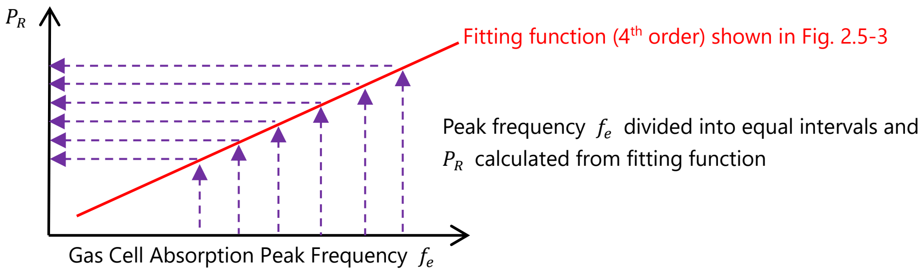

(a) Phase of Reference Signal P_R Calculated from Fitting Function

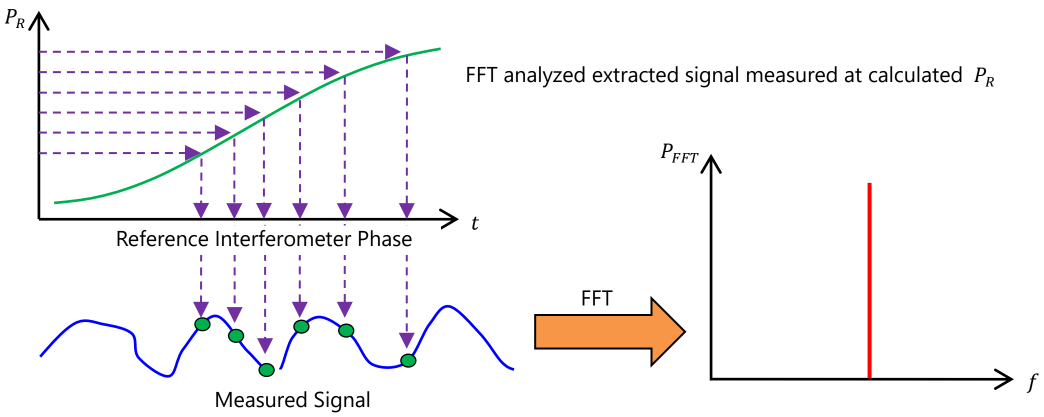

(b) Measured Signal Calculated from Reference Interference Signal

Fig. 2.5-4 Example of Sampling Measured Signal Calculated from Gas Cell Absorption Peak Frequency and FFT Analysis Result

If $\Delta \boldsymbol{P_R}$ represents the change in $\boldsymbol{P_R}$ when frequency changes by $\Delta \boldsymbol{\nu}$, the FSR for the resonator length of the reference interference is expressed by the following equation.

$$FSR = \frac{\Delta \nu}{\Delta P_R/(2\pi)} \tag{22}$$

Since the resonator length $\boldsymbol{L_{AUX}}$ can be expressed by the following equation, where *c* is the velocity of light,

$$L_{AUX} = \frac{c}{2FSR} \tag{23}$$

and since $\Delta \boldsymbol{P_R}/(\boldsymbol{2\pi})$ is the number of phase rotations, the resolution $\Delta \boldsymbol{z}$ can be found from the following derivation.

$$\Delta z = \frac{L_{AUX}}{\Delta P_R/(2\pi)} = \frac{c}{2\Delta \nu} = \frac{\lambda_c^2}{2\Delta\lambda} \tag{24}$$

If FFT analysis is performed with the equally divided number as N (= power of 2), the longest measurement length $\boldsymbol{z_{max}}$ can be expressed by the following equation.

$$z_{max} = \Delta z \cdot N/2 \tag{25}$$

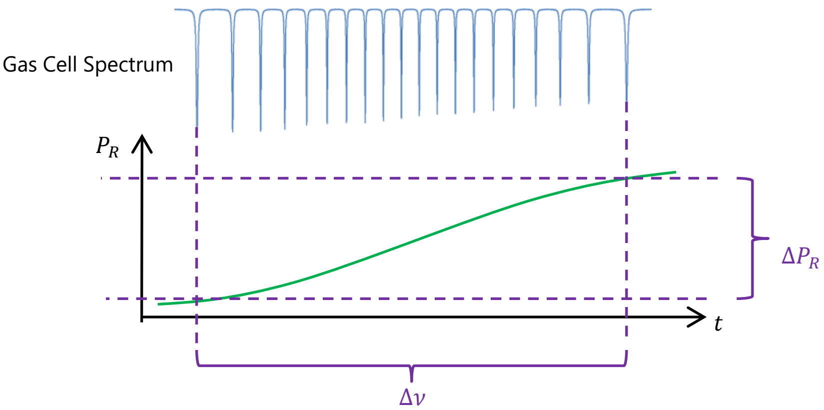

Fig. 2.5-5 Relationship Between Optical Frequency and Phase

2.6 Optical Path Length Difference Measurement of Reference Interferometer

Section 2.3.1 explained the approach for the reference optical path length difference L_{AUX} regarding distance to the measurement target. For example, when the distance from the collimator lens to the measurement target is 10 m, the return optical path length difference is 20 m. At this time, the reference interferometer optical path length difference L_{AUX} must be twice 20 m (40 m for return) from the viewpoint of the Nyquist frequency at FFT analysis. The minimum required length of optical fiber can be calculated easily by determining the reference interferometer optical path length difference L_{AUX} from the distance to measurement target. By measuring the optical path length difference L_{AUX} more accurately, the maximum measurement distance at FFT analysis can be found, which can be used to accurately calculate the position of the reflection using proportional calculation. To measure the reference interferometer path length, it is necessary to sample the wavelength reference signal simultaneously with the interference signal obtained from the measurement target. By using our wavelength swept light sources, this is achieved by sampling the measured data at the same time as the reference wavelength signal from the etalon. The etalon peak wavelength is very precise and is measured beforehand. By using this value, the etalon peak position, or in other words, the sampling position, is plotted on the x-axis and the optical frequency calculated from the etalon peak wavelength is plotted on the vertical axis. Figure 2.6-1 shows an example of the results. In this example, the wavelength sweep width is set to 20 nm. Etalon peaks are found at five positions. By plotting the etalon peak sampling positions on the x-axis and the etalon frequency on the y-axis, the gradient can be found using the least-squares method and the reference interferometer FSR can be calculated. The reference interference signal optical path length is calculated using this FSR calculation. As an example, when the reference interferometer optical path length is 8 m, the reference interferometer optical path length is calculated to be 1,1870.710 mm using the following Eq. (27). If the refractive index of the optical fiber is 1.46, the reference interferometer optical path length difference is calculated as 8,130.623 mm. Since this is the length of the return path to and from the measurement target, the maximum measurement distance is half this value or 4,065.3115 mm, and the position (maximum measurement distance) of the data at the right edge at FFT analysis is equivalent to this value. However, because the maximum measurement distance can change due to the impact of external effects, such as temperature changes during measurement, this calculation should be performed at each sweep.

$$\nu_{etalon} = FSR \times N_{etalon} + \alpha \qquad (26)$$

$$FSR = \frac{c}{2nL_{AUX}} \qquad (27)$$

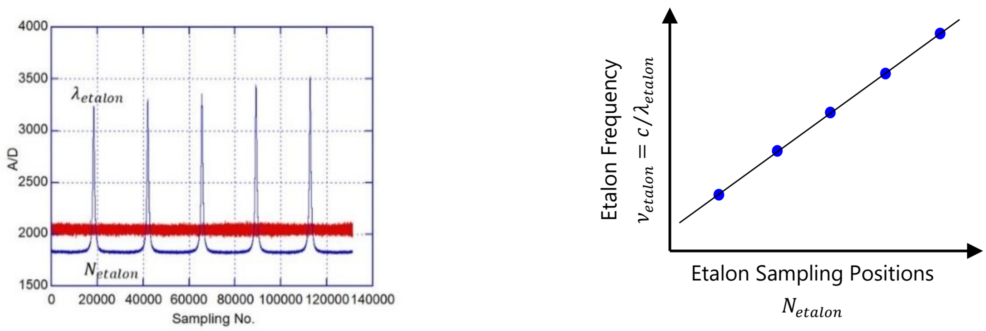

Fig. 2.6-1 Example of Reference Interferometer Optical Path Length Difference Measurement Result

2.7 Peak Detection

Figure 2.7-1(a) shows an example of FFT analysis results. The Angled Physical Contact (APC) end face of the optical fiber connected to the collimator lens, the collimator lens face, and the peak reflected from the measurement target can all be seen. The peak near 800 mm is the peak reflection from the end face of the optical fiber connector at the OFDR system chassis described later (Fig. 3-1). The position of the distance origin (frequency 0) calculated from the FFT results is the same for both the reference optical path length and the measurement optical path length, but this position can change due to the effect of the external environment, such as the temperature of the optical fiber. Therefore, the reflection peak from the APC end face of the fiber connected to the collimator lens appears as the measured signal and this position is used as the origin of the distance measurement to the measurement target. The signal drops below the noise floor on the horizontal distance axis near 4,300 mm but this is due to the effect of the optical receiver bandwidth.

The peak waveform data obtained by FFT analysis is distributed making it difficult to evaluate the peak position consistently at each measurement because a different waveform may be captured at each measurement. Therefore, appropriate computation processing is applied to the measured data for consistent detection of the peak position. Figure 2.7-1(b) shows the concept of the required peak position detection processing. First, the detected peak waveform is subjected to moving average processing to produce a single peak (solid red line). Next, differentiation is applied to the moving-average waveform (solid green line). Then linear approximation is applied to the peak wavelength range to find the peak position consistently and accurately by detecting the position where the differentiated waveform value becomes 0 as the peak. As a result of this procedure the peak position is detected with both high accuracy and consistency.

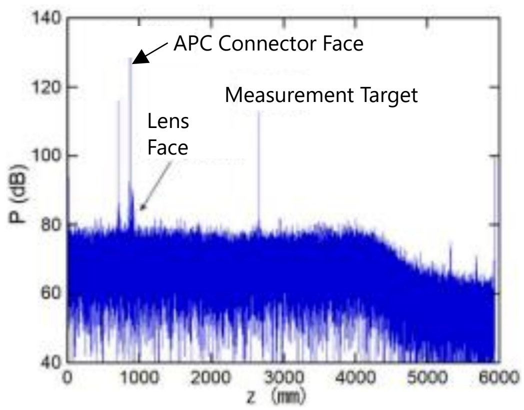

(a) Example of FFT Analysis Results

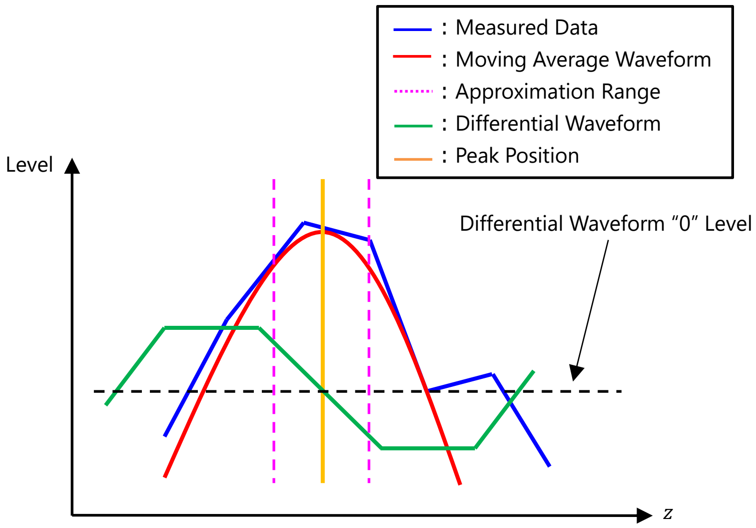

(b) Explanation of Peak Position Detection

Fig. 2.7-1 Peak Position Detection

2.8 Distance Calculation

The accurate peak detected plotted on the x-axis as described in section 2.7 is converted to distance. Figure 2.8-1 shows the results of FFT analysis by sampling 131,072 (2^{17}) data points. Based on these results, when the reference interferometer optical path length is 8 m, the distance of the data at half the sample (65,636 or 2^{16}) is half the delay length distance (11,870.710 mm). Consequently, in this case, when the refractive index of the optical fiber is 1.46, the value becomes 4,065.3115 m. Clarification of this position facilitates clarification of the peak position by proportional calculation.

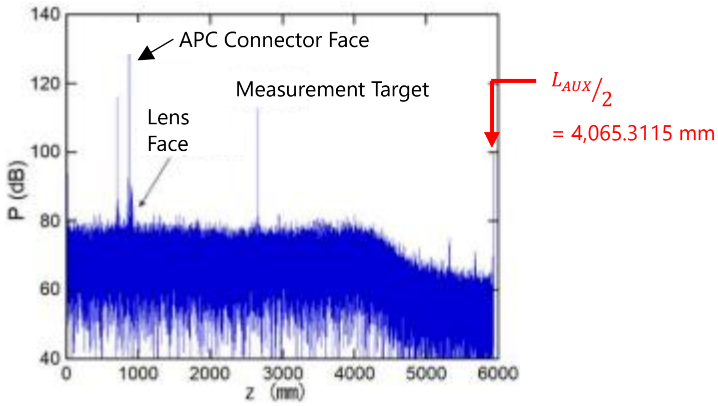

Fig. 2.8-1 FFT Analysis Result

2.9 Wavelength Sweep Width and Resolution

This section explains the relationship between the wavelength sweep width used for measurement and the measurement resolution. As an example, Fig. 2.9-1(a) shows the measurement results when measuring the distance to the measurement target using131,072 (2^{17}) sampling points with a sweep width of 13 nm; Fig. 2.9-1(b) shows a magnified view of the circled highlight in (a). The optical frequency width is 1.6 THz at a sweep width of 13 nm (±6.5 nm) for a center wavelength of 1550 nm. In this case, based on the Eq. (12) theoretical resolution, the peak has a calculated as a peak with a full width at half maximum of 92 µm. The actual peak with a full width at half maximum measured result of 100 µm is a good match within about 10% of this value.

Next. Fig. 2.9-2(a) shows the measurement result when measuring with a wavelength sweep width of 26 nm or twice the above measurement; Fig. 2.9-2(b) shows a magnified view of the circled highlight in (a). In this case, the optical frequency width is 3.2 THz. However, although the wavelength sweep width is doubled, each sample point is decimated because the same number of samples is measured. Although the theoretical resolution in this case is 46 µm, as shown in the magnified view in Fig. 2.9-2(b), the resolution is about 50 µm, which is also a good match in this case. However, comparing the measurement results in Fig. 2.9-2(a) with Fig. 2.9-1(a), the latter measured distance is half that of the former distance because the distance resolution is halved for the same number of samples. This is equivalent to decimating the data by halving the sampling bandwidth.

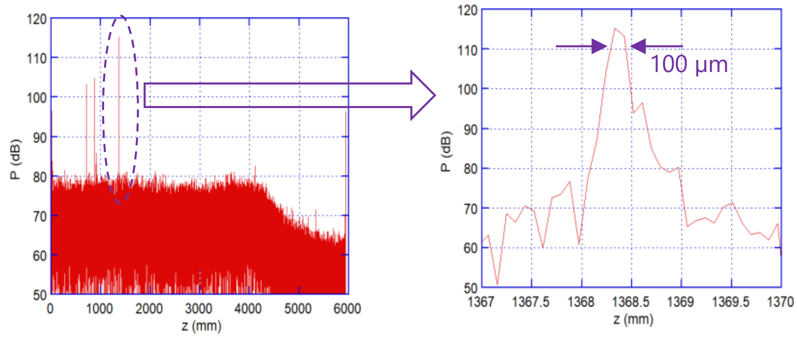

(a) Measurement Result (b) Magnified Peak Part

Fig. 2.9-1 Distance Measurement Result for 13 nm Wavelength Sweep Width Setting

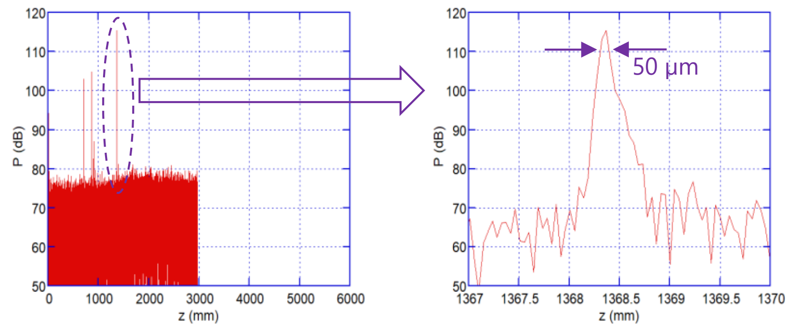

(a) Measurement Result (b) Magnified Peak Part

Fig. 2.9-2 Distance Measurement Result for 26 nm Wavelength Sweep Width Setting

2.10 Temporal variation in distance measurement

This section describes temporal variation in distance measurement. To confirm the actual change amount, the measurement target was positioned at a distance of about 540 mm from the collimator lens and the wavelength sweep width was set to 20 nm. Figure 2.10-1 shows the measurement results. The result standard deviation was about 0.2 μm at repeated measurement every 10 s. Although the theoretical resolution was about 60 μm, the measured detection accuracy of the reflected peak position on the FFT spectrum was much higher than this.

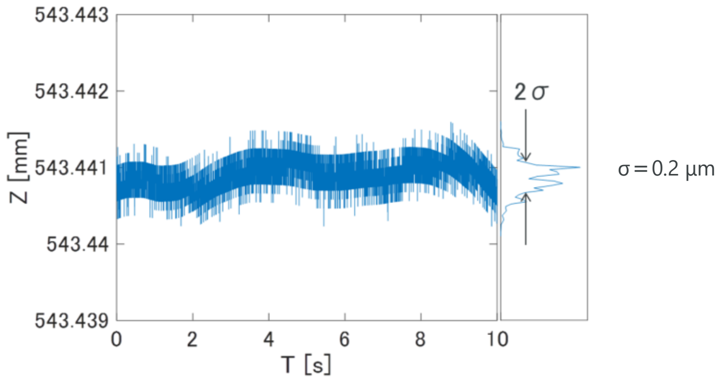

Fig. 2.10-1　Temporal variation in distance measurement

3 Measurement Examples

The OFDR measurement system explained up to Chapter 2 is actually configured and the surface shape is measured. Figure 3-1(a) shows the actual appearance of the configured system and Fig. 3-1(b) shows the internal configuration. For portability, the wavelength swept light source, optical interferometer and optical receiver are housed in a chassis. The optical interferometer uses a Mach-Zehnder design without an optical circulator. The chassis also houses an A/D conversion board for data processing, and an automatic stage controller for 2D collimator lens scanning. Additionally, an optical coupler in the optical interferometer section is provided for input light from a red LED for output from the collimator lens as a visible marker indicating the current scanning position. The red LED wavelength has no impact on the surface shape measurement results. The sampling data is analyzed at the A/D conversion board and the results are transferred via a high-speed Thunderbolt 3 interface for display at the external PC not housed in the chassis. The selected PC has a built-in, high-performance GPU for high-speed data processing. Since the optical interferometer collimator lens must scan the measurement target position, it is mounted outside the chassis on a tripod stage controlled by signals from the automatic stage controller in the chassis. The A/D conversion board, collimator lens, automatic stage controller, etc., are all freely available on the commercial market.

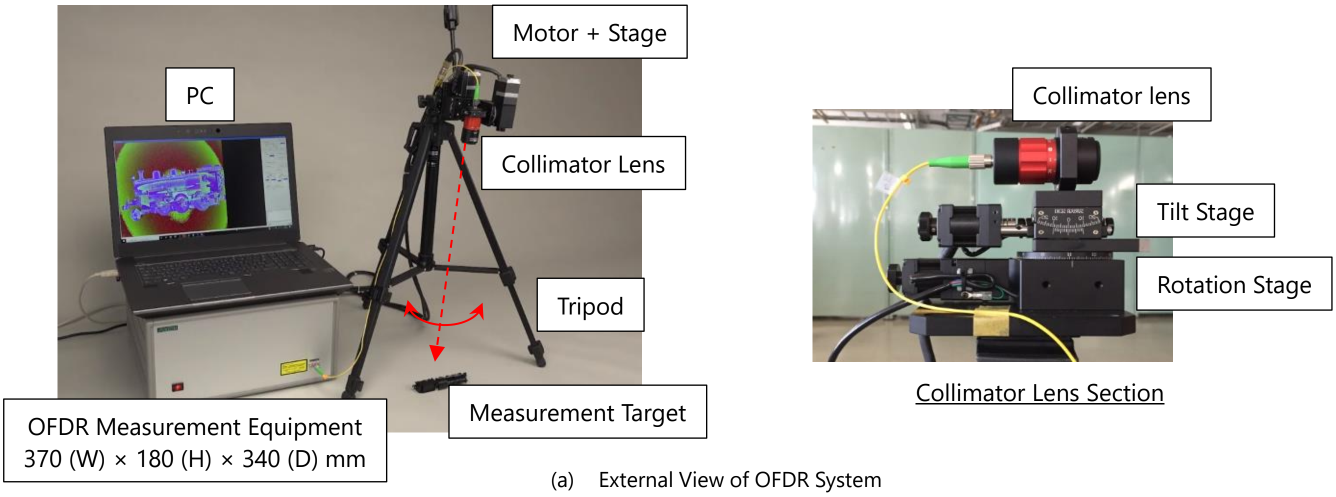

(a) External View of OFDR System

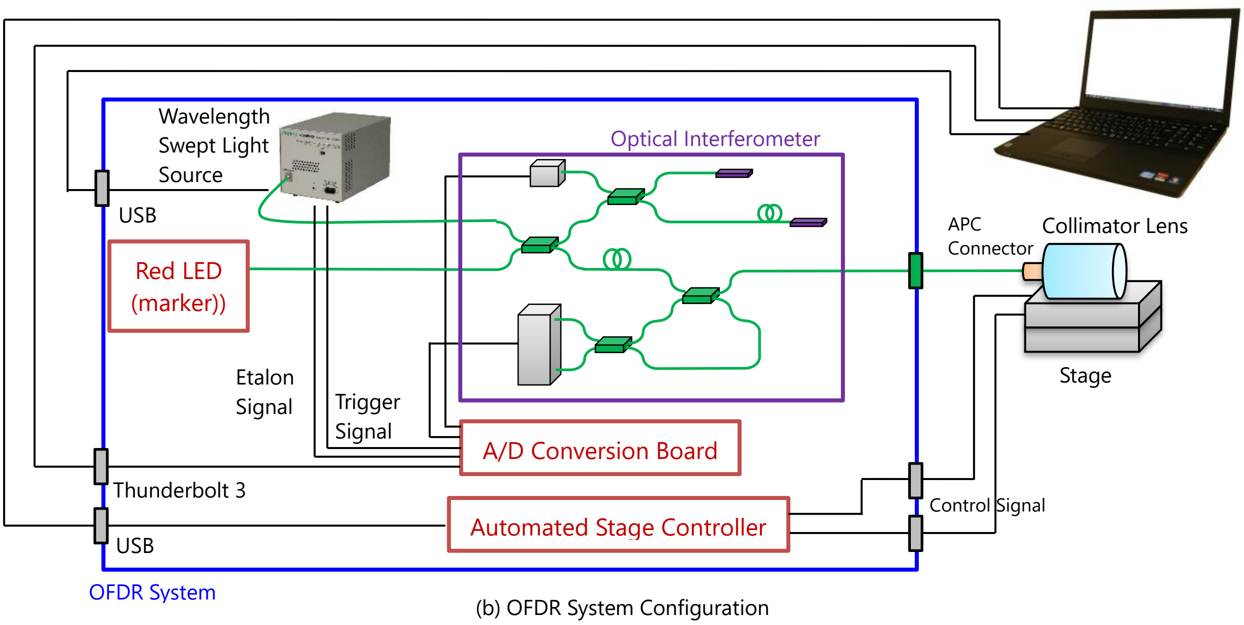

(b) OFDR System Configuration

Fig. 3-1 Prototype OFDR System Configuration

3.1 Car Body Surface Shape Measurement

This section explains measurement of the surface shape of a car body as a relatively large object using the OFDR system shown in Fig. 3-1. The car body dimensions are about 1.5 (H) × 4.4 (W) m. The Anritsu Wavelength Swept Light Source AQA5500P with a sweep frequency of 1250 Hz was used for measurement. The sweep width was 15 nm and sampling was performed over the central 10-nm range with high linearity. As a result, the theoretical resolution was 120 µm. In addition, the reference interferometer delay length ΔL_{AUX} was 10 m for a distance to the measurement target of 4.5 m. Consequently, the maximum measurable distance was about 7.3 m (10 m/2 x 1.46 (refractive index)). Additionally, the reference signal frequency f_{Beat} was about 700 MHz. Hardware linearization processing was used for sampling measured data.

At measurement close to a large target, since there are large differences in distances to different parts of the target, it is difficult to perform delay calibration as described in section 2.4 for all data from the large surface. Consequently, the OFDR system collimator lens was positioned 4.5 m from the car body and the automatic stage was used to perform scanning through 24° vertically and 54° horizontally to measure a vertical range of 1.9 m and a horizontal range of 4.6 m.

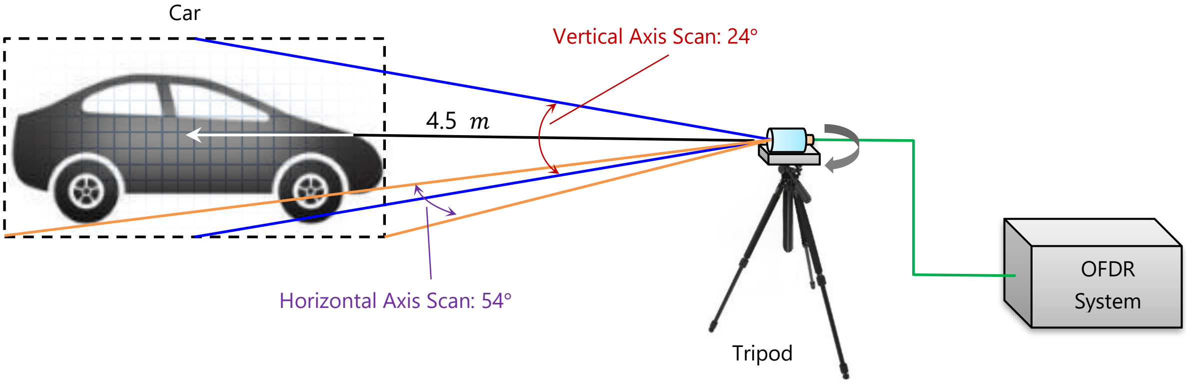

Fig. 3.1-1 Car Body Surface Shape Measurement System

At actual measurement, it is essential to select the optimum distance to the measurement, the wavelength sweep width the measurement resolution, and the A/D conversion board sampling frequency. When setting a wide sweep width and increasing resolution to measure at higher accuracy, the sampling frequency becomes higher, requiring a sampling frequency higher than the A/D conversion board specifications. To reduce the sampling frequency, it is necessary to set a smaller reference interferometer delay length ΔL_{AUX} but this shortens the measurement range. To achieve the best setting for this, first, determine the reference interferometer delay length ΔL_{AUX} by considering the distance to the measurement target and then pay attention to the relationship between the sampling number and measurement resolution to determine the optimum wavelength sweep width for the A/D conversion board sampling frequency.

When measuring the shape of the car side, first, fixed point measurement near the door of the car body was carried out. Figure 3.1-2 shows the result for a 10-s measurement with the collimator lens at a fixed position. Since the measurement was made outdoors, the car body was vibrating due to the effect of external factors, such as wind, and the measured data shows some dispersion with a standard deviation (σ) value of 5.6 µm.

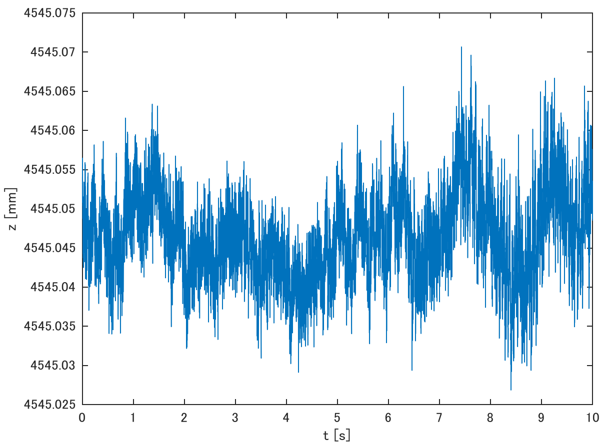

Fig. 3.1-2 Results of Observation of Fixed Point Near Car Door

Figure 3.1-3(a) is a photograph of the vehicle used for measurement and Fig. 3.1-3(b) shows the surface shape measurement results, which are displayed using the MATLAB analysis software. The display is 500 × 500 pixels. Instead of moving the OFDR system position around the measurement target car, the entire vehicle surface shape was measured as one set of scans, requiring a time of about 12 minutes. Figures 3.1-3(c) to (e) show cross-section scans near the center of the car body. Figure 3.1-3(e) is a magnified view of the circled part in (d) with a 50-μm ripple, confirming the ability to measure at high accuracy from a distance.

(a) Car Body

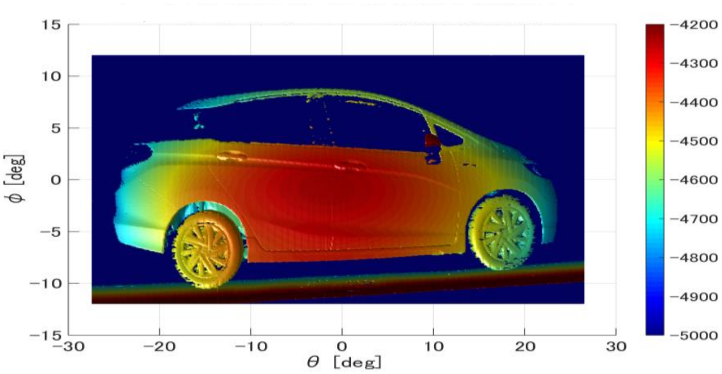

(b) Body Surface Shape Measurement Result

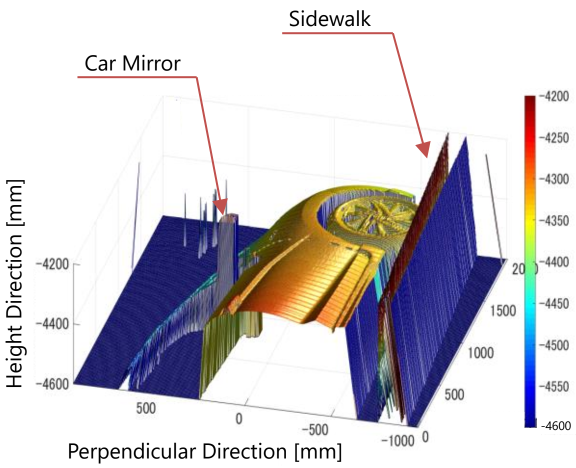

(c) Cross-section Near Body Center

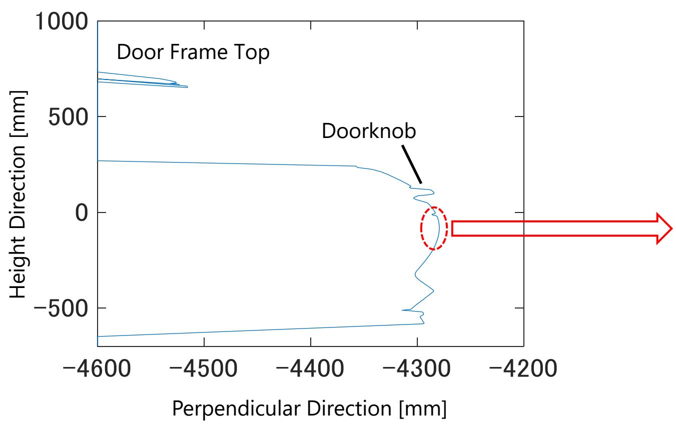

(d) Cross-section Near Body Center

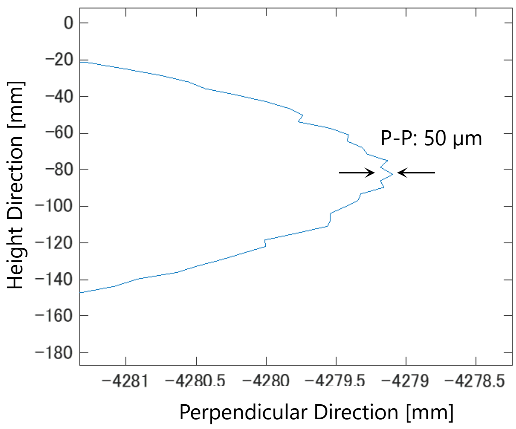

(e) Magnified Circle in (d)

Fig. 3.1-3 Body Surface Measurement Results

3.2 Gage Block Surface Shape Measurement

This section uses measurement of a gage block with fine steps to demonstrate high-accuracy measurement of a small measurement target from a short distance. The Mitsutoyo gage block with fine steps of 0.25, 0.5, 1.0 and 2.0 µm is used as a mask. The Anritsu Wavelength Swept Light Source AQA5500P (sweep frequency of 1250 Hz) was used for measurement and the sweep width was set to the maximum of 110 nm for this light source to achieve the best possible resolution; the central 104 nm range with the highest linearity was used for sampling. As a result, the theoretical resolution was 12 µm. Although a high resolution was used for the gage block steps, it was still possible to calculate the reflection peak positions with high accuracy using the peak detection method described in section 2.7. Moreover, the reference interference delay length ΔL_{AUX} was 2 m for a distance of about 137 mm from the fiber connector end face to the gage block measurement target. Consequently, the maximum measurable distance was 1.5 m (2 m/2 x 1.46 (refractive index)). The reference interference signal frequency f_{Beat} was about 1 GHz. Hardware linearize processing was used to sample the measured data. At measurement of the car body pictured in section 3.1, the collimator lens performed 2D scanning using an automatic stage, but in this measurement, the gage block was mounted on the stage for 2D scanning (Fig. 3.2-1(a).

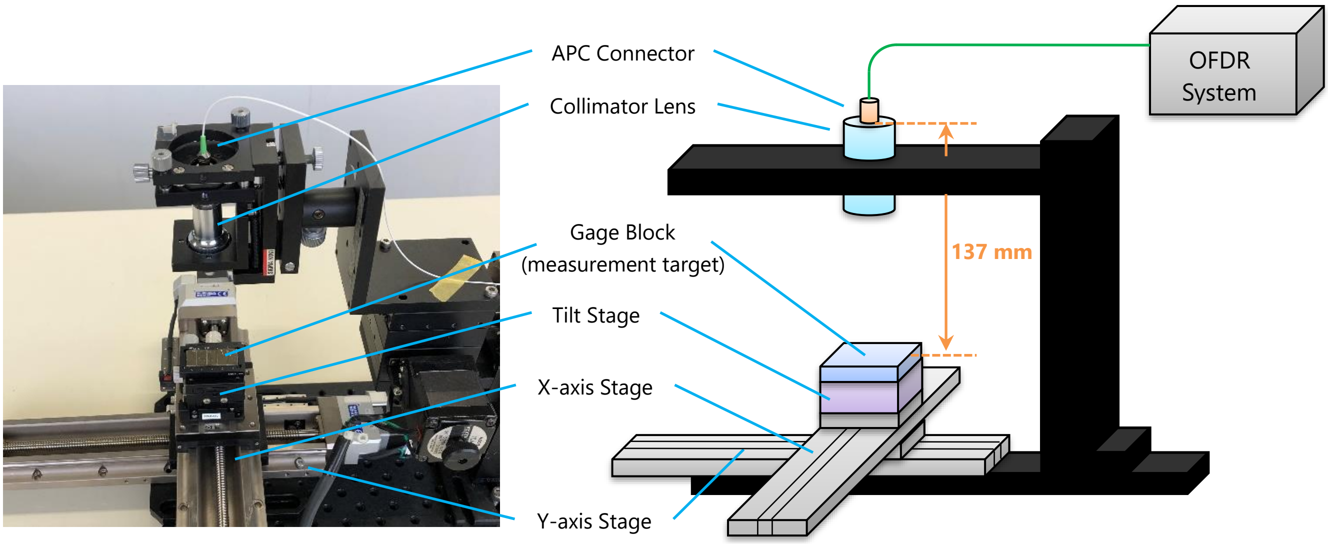

(a) Gage Block Measurement System

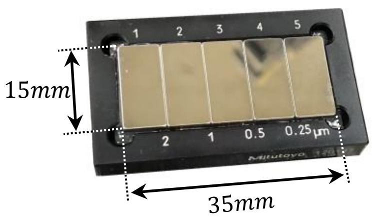

(b) Gage Block Appearance

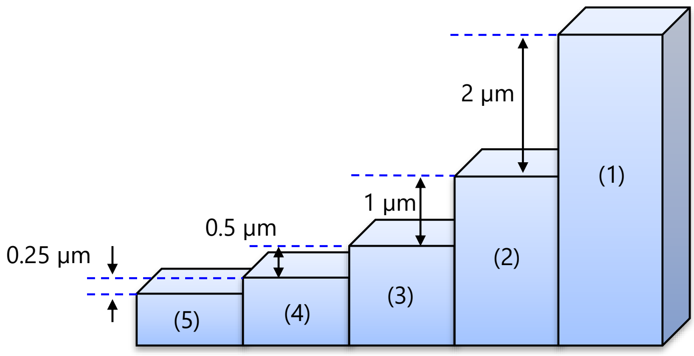

(c) Gage Block Steps

Fig. 3.2-1 Gage Block Measurement System and External Appearance

Figure 3.2-2(a) shows the surface shape measurement results. Five-hundred samples were measured in the y-axis direction (step direction) and 125 samples were made in the x-axis direction with a measurement time of about 5 minutes. Figure 3.2-2(b) shows the results of measurement near the center of the x-axis. The steps are shown from step (3), setting the height of center step (3) as the 0 index. Table 3.2-1 lists the maker's gage block step specifications and the results measured by OFDR. The maximum difference between the two data sets is 0.14 μm, confirming the ability to measure fine steps with high accuracy.

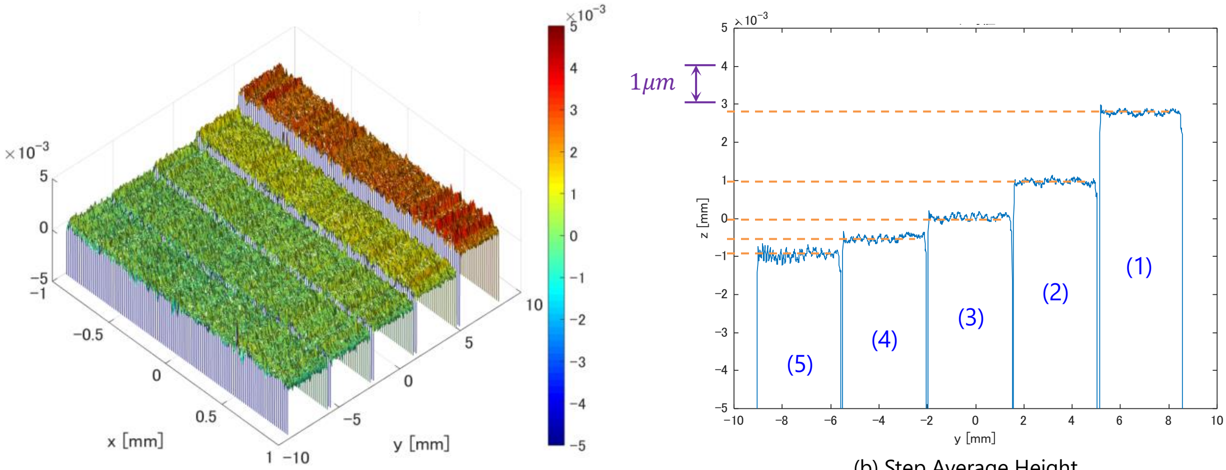

(a) Step Measurement Results

(b) Step Average Height

Fig. 3.2-2　Gage Block Measurement Results

Table 3.2-1　Maker's Specifications and Measured Step Differences

	(5)	(4)	(3)	(2)	(1)
Step (μm)	−0.75	−0.5	0	1.0	3.0
Maker Specified Value (μm)	−0.83	−0.49	0	1.0	2.94
OFDR Measured Value (μm)	−0.9	−0.5	0	1.0	2.8
Difference (μm)	0.07	0.01	0	0	0.14

4 Conclusions

We have explained the configuration of an OFDR measurement system using a wavelength swept light source as well as the measurement procedure, the method for calibrating nonlinearity in the optical signal from the light source using hardware linearize processing and software linearize processing procedures, the wavelength dispersion compensation method, and the peak position detection method. Moreover, we have described large distance measurement of the surface shape of a large car in one scan series without moving the measurement system around the vehicle. Additionally, we have demonstrated the ability to short distance measure a gage block with fine steps of less than 1-μm height at high accuracy.

Please refer to our published "Application NOTE " for the results of other shape measurements. For example, the results of hole bottom shape measurement of deep hole parts, which are difficult to measure by contact type or camera type measurement, and the shape measurement results of train track models with complicated structures are described. It also describes other applications that are expected to be applied.

5 References

1） K. Nakamura, S. Morimoto, and T. Nakayama, "Single-Mode and Mode-Hop-Free Wavelength Sweep Light Source with Range of Over 160 nm and High Swept Frequency," IEEE Photonics Technology Letters, Vol. 22, No. 19, Oct. 2010.

2） K. Nakamura, M. Koshihara, T. Saitoh, and K. Kawakita，"High-Coherence Wavelength Swept Light Source"，Anritsu Technical Review No.25

3） T. Saitoh,"3D Shape Measurement Using OFDR"，Anritsu Technical Review No.28

4） T. Saitoh，"High Precision Shape Measurement using High Coherence Wavelength Swept Light Source"，IEICE Technical Report, OFT2020-43(2020-11).

Advancing beyond

Please contact following local office for the quotation and order.
Anritsu Corporation reserves the right to change the content of the catalog at any time without notice.

ANRITSU CORPORATION
SENSING & DEVICES COMPANY
OVERSEAS SALES DEPT

Tel +81 46 296 6783 fax +81 46 225 8390
5-1-1 Onna, Atsugi-shi, Kanagawa
243-8555 Japan

URL: https://www.anritsu.com/sensing-devices